



- (51) **International Patent Classification:**  
A61N 7/00 (2006.01) A61B 17/225 (2006.01)
- (21) **International Application Number:**  
PCT/US2021/048008
- (22) **International Filing Date:**  
27 August 2021 (27.08.2021)
- (25) **Filing Language:** English
- (26) **Publication Language:** English
- (30) **Priority Data:**  
63/071,301 27 August 2020 (27.08.2020) US
- (71) **Applicant: THE REGENTS OF UNIVERSITY OF MICHIGAN [US/US];** Office of Technology Transfer, 1600 Huron Parkway, 2nd Floor, Ann Arbor, MI 48109-2590 (US).
- (72) **Inventors: HALL, Timothy, Lewis;** Office of Technology Transfer, 1600 Huron Parkway, 2nd Floor, Ann Arbor, MI 48109-2590 (US). **SUKOVICH, Jonathan, Robert;** Office of Technology Transfer, 1600 Huron Parkway, 2nd Floor, Ann Arbor, MI 48109-2590 (US). **XU, Zhen;** Office of Technology Transfer, 1600 Huron Parkway, 2nd Floor, Ann Arbor, MI 48109-2590 (US). **MACOSKEY, Jonathan, Jenner;** Office of Technology Transfer, 1600 Huron Parkway, 2nd Floor, Ann Arbor, MI 48109-2590 (US).
- (74) **Agent: THOMAS, Justin et al.;** Shay Glenn LLP, 2929 Campus Drive, Suite 225, San Mateo, CA 94403 (US).

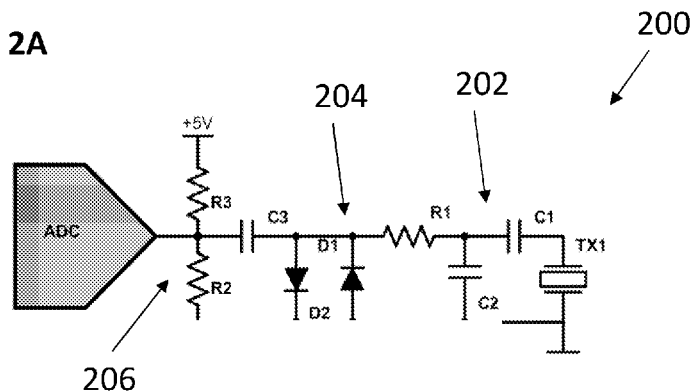
- (81) **Designated States** (unless otherwise indicated, for every kind of national protection available): AE, AG, AL, AM, AO, AT, AU, AZ, BA, BB, BG, BH, BN, BR, BW, BY, BZ, CA, CH, CL, CN, CO, CR, CU, CZ, DE, DJ, DK, DM, DO, DZ, EC, EE, EG, ES, FI, GB, GD, GE, GH, GM, GT, HN, HR, HU, ID, IL, IN, IR, IS, IT, JO, JP, KE, KG, KH, KN, KP, KR, KW, KZ, LA, LC, LK, LR, LS, LU, LY, MA, MD, ME, MG, MK, MN, MW, MX, MY, MZ, NA, NG, NI, NO, NZ, OM, PA, PE, PG, PH, PL, PT, QA, RO, RS, RU, RW, SA, SC, SD, SE, SG, SK, SL, ST, SV, SY, TH, TJ, TM, TN, TR, TT, TZ, UA, UG, US, UZ, VC, VN, WS, ZA, ZM, ZW.
- (84) **Designated States** (unless otherwise indicated, for every kind of regional protection available): ARIPO (BW, GH, GM, KE, LR, LS, MW, MZ, NA, RW, SD, SL, ST, SZ, TZ, UG, ZM, ZW), Eurasian (AM, AZ, BY, KG, KZ, RU, TJ, TM), European (AL, AT, BE, BG, CH, CY, CZ, DE, DK, EE, ES, FI, FR, GB, GR, HR, HU, IE, IS, IT, LT, LU, LV, MC, MK, MT, NL, NO, PL, PT, RO, RS, SE, SI, SK, SM, TR), OAPI (BF, BJ, CF, CG, CI, CM, GA, GN, GQ, GW, KM, ML, MR, NE, SN, TD, TG).

**Published:**

- with international search report (Art. 21(3))
- before the expiration of the time limit for amending the claims and to be republished in the event of receipt of amendments (Rule 48.2(h))

(54) **Title:** ULTRASOUND TRANSDUCER WITH TRANSMIT-RECEIVE CAPABILITY FOR HISTOTRIPSY

**FIG. 2A**



(57) **Abstract:** A histotripsy therapy system configured for the treatment of tissue is provided, which may include any number of features. Provided herein are systems and methods that provide efficacious non-invasive and minimally invasive therapeutic, diagnostic and research procedures. In particular, provided herein are optimized systems and methods that provide targeted, efficacious histotripsy in a variety of different regions and under a variety of different conditions without causing undesired tissue damage to intervening/non-target tissues or structures.

WO 2022/047193 A1

**ULTRASOUND TRANSDUCER WITH TRANSMIT-RECEIVE  
CAPABILITY FOR HISTOTRIPSY**

**CROSS REFERENCE TO RELATED APPLICATIONS**

5    **[0001]**     This application claims the benefit of US Provisional Patent Application No. 63/071,301, filed August 27, 2020, titled “ULTRASOUND TRANSDUCER WITH TRANSMIT-RECEIVE CAPABILITY FOR HISTOTRIPSY”, which is incorporated by reference in its entirety.

10

**GOVERNMENT RIGHTS**

**[0002]**     This invention was made with government support under CA211217, EB028309, and NS108042 awarded by the National Institutes of Health and under N00014-17-1-2058 and N00014-18-1-2625 awarded by the U.S. Office of Naval Research. The government has certain rights in the invention.

15

**INCORPORATION BY REFERENCE**

**[0003]**     All publications and patent applications mentioned in this specification are herein incorporated by reference to the same extent as if each individual publication or patent application was specifically and individually indicated to be incorporated by reference.

20

**FIELD**

**[0004]**     The present disclosure details novel histotripsy systems configured to produce acoustic cavitation, methods, devices and procedures for the minimally and non-invasive treatment of healthy, diseased and/or injured tissue. The histotripsy systems and methods described herein, also referred to Histotripsy, may include transducers, drive electronics, 25 positioning robotics, imaging systems, and integrated treatment planning and control software to provide comprehensive treatment and therapy for soft tissues in a patient.

**BACKGROUND**

30   **[0005]**     Many medical conditions require invasive surgical interventions. Invasive procedures often involve incisions, trauma to muscles, nerves and tissues, bleeding, scarring, trauma to organs, pain, need for narcotics during and following procedures, hospital stays, and risks of infection. Non-invasive and minimally invasive procedures are often favored, if available, to avoid or reduce such issues. Unfortunately, non-invasive and minimally invasive

procedures may lack the precision, efficacy or safety required for treatment of many types of diseases and conditions. Enhanced non-invasive and minimally invasive procedures are needed, preferably not requiring ionizing or thermal energy for therapeutic effect.

5 [0006] Histotripsy, or pulsed ultrasound cavitation therapy, is a technology where extremely short, intense bursts of acoustic energy induce controlled cavitation (microbubble formation) within the focal volume. The vigorous expansion and collapse of these microbubbles mechanically homogenizes cells and tissue structures within the focal volume. This is a very different end result than the coagulative necrosis characteristic of thermal ablation. To operate within a non-thermal, Histotripsy realm; it is necessary to deliver acoustic energy in the form of  
10 high amplitude acoustic pulses with low duty cycle.

[0007] Compared with conventional focused ultrasound technologies, Histotripsy has important advantages: 1) the destructive process at the focus is mechanical, not thermal; 2) cavitation appears bright on ultrasound imaging thereby confirming correct targeting and localization of treatment; 3) treated tissue generally, but not always, appears darker (more  
15 hypoechoic) on ultrasound imaging, so that the operator knows what has been treated; and 4) Histotripsy produces lesions in a controlled and precise manner. It is important to emphasize that unlike thermal ablative technologies such as microwave, radiofrequency, and high-intensity focused ultrasound (HIFU), Histotripsy relies on the mechanical action of cavitation for tissue destruction.

20

### BRIEF DESCRIPTION OF THE DRAWINGS

[0008] The novel features of the invention are set forth with particularity in the claims that follow. A better understanding of the features and advantages of the present invention will be obtained by reference to the following detailed description that sets forth illustrative  
25 embodiments, in which the principles of the invention are utilized, and the accompanying drawings of which:

[0009] FIGS. 1A-1B illustrate an ultrasound imaging and therapy system.

[0010] FIGS. 2A-2D illustrate various schematic illustrations of transmit-receive drive electronics for a histotripsy system.

30 [0011] FIGS. 3A-3C are embodiments of current sense electronics for a histotripsy system.

[0012] FIG. 4 is a method of providing histotripsy therapy to a patient.

[0013] FIG. 5 illustrates cavitation mapping through bone such as a human skull.

[0014] FIG. 6 is a method of providing histotripsy therapy to a patient.

**[0015]** FIGS. 7-10 illustrate data collected via received ultrasound signals from histotripsy therapy to predict treatment progress and tissue fractionation.

### SUMMARY OF THE DISCLOSURE

- 5 **[0016]** Histotripsy produces tissue fractionation through dense energetic bubble clouds generated by short, high-pressure, ultrasound pulses. When using pulses shorter than 2 cycles, the generation of these energetic bubble clouds only depends on where the peak negative pressure ( $P_-$ ) exceeds an intrinsic threshold for inducing cavitation in a medium (typically 26 – 30 MPa in soft tissue with high water content).
- 10 **[0017]** A transmit-receive driving electronics for a histotripsy system is provided, comprising at least one transducer element configured to transmit ultrasound pulses in a transmit mode and receive ultrasound reflections and/or acoustic cavitation emissions in a receive mode, a current sense resistor configured to measure a current in the transmit-receive driving electronics during the receive mode, a bypass circuit electrically coupled to the at least one transducer
- 15 element and the current sense resistor, wherein the bypass circuit is configured to be switched on during the transmit mode to bypass the current sense resistor and switched off during the receive mode to allow the sense resistor to measure the current; a gain adjustment circuit electrically coupled to the current sense resistor and to a low sensitivity resistor, the gain adjustment circuit being configured to operate in a high sensitivity setting in which the current sense resistor is
- 20 switched on and the low sensitivity resistor is switched off, and wherein the gain adjustment circuit is further configured to operate in a low sensitivity setting in which the current sense resistor and the low sensitivity resistor are switched on.
- [0018]** In some embodiments, the transmit-receive driving electronics further comprises a drive transformer electrically coupled to the at least one transducer element.
- 25 **[0019]** In some examples, the bypass circuit further comprises a pair of bypass transistors. In other embodiments, the bypass circuit further comprises a pair of bypass diodes.
- [0020]** In some embodiments, the gain adjustment circuit further comprises a pair of transistors. In other embodiments, the current sense resistor has a higher resistance than the low sensitivity resistor.
- 30 **[0021]** In one example, the current sense resistor has a resistance of approximately 200 ohms and the low sensitivity resistor has a resistance of approximately 5 ohms.
- [0022]** A transmit-receive driving electronics for a histotripsy system is also provided, comprising an ultrasound transducer array, high-voltage transmission electronics coupled to the ultrasound transducer array and configured to provide up to thousands of volts to the ultrasound

transducer array to produce one or more histotripsy pulses, first receive electronics coupled to the ultrasound transducer array and configured to receive incoming voltage signals from the transmitted one or more histotripsy pulses, the first receive electronics being configured to attenuate the incoming voltage signals by 90-99%, second receive electronics configured to compress any attenuated incoming voltage signals above 1V, and third receive electronics configured to voltage shift the attenuated incoming voltage signals, and an analog-to-digital converter configured to receive the voltage-shifted attenuated incoming voltage signals from the third receive electronics for ADC conversion.

**[0023]** In some embodiments, the first electronics comprise a voltage divider.

10 **[0024]** In other embodiments, the voltage divider comprises a capacitive voltage divider.

**[0025]** In one embodiment, the capacitive voltage divider comprises a first capacitor and a second capacitor in parallel with a first transducer element of the ultrasound transducer array.

**[0026]** In one embodiment, the second receive electronics comprise a diode-resistor voltage divider. In another embodiment, the third receive electronics are configured to voltage shift the attenuated incoming voltage signals to an appropriate voltage range for the analog-to-digital converter.

**[0027]** In some embodiments, the transmit-driving electronics comprise a separate circuitry board that is configured to be retrofitted to an existing histotripsy system that includes a transmit-only histotripsy driving system.

20 **[0028]** In one example, the transmit-driving electronics is added in parallel to the transmit-only histotripsy driving system and is configured to passively receive signals without affecting the transmit-only electronics.

**[0029]** In some embodiments, the transmit-receive driving electronics are further configured to synchronize a time clock of the transmitted one or more histotripsy pulses, received incoming voltage signals, and the ADC conversion to obtain an appropriate time window after each histotripsy pulse transmission.

**[0030]** In one embodiment, the transmit-receive driving electronics further comprise one or more Field Programmable Gate Array (FPGA) boards coupled to the analog-to-digital converter and being configured to control transmit and receive operations of the transmit-receive driving electronics with a single clock. In some examples, the one or more FPGA includes software or firmware configured to reduce a data load for received signals. In other embodiments, the one or more FPGA are configured to artificially downsample incoming data from the analog-to-digital converter. In another embodiment, the one or more FPGA are configured to oversample and average the received signals to increase a signal to noise ratio (SNR).

**[0031]** A method of using a transmit-receive histotripsy system for cavitation detection is provided, comprising the steps of transmitting high-voltage histotripsy therapy pulses into a target tissue with transmit electronics and a histotripsy therapy transducer array to generate cavitation in the target tissue, receiving low-voltage acoustic cavitation emission signals from the cavitation with receive electronics and the histotripsy therapy transducer array, processing the received acoustic cavitation emission signals to monitor treatment progression.

**[0032]** In some examples, the method further comprises generating a 3D map of cavitation produced by the transmitted pulses in real-time.

**[0033]** A method of using a transmit-receive histotripsy system for aberration correction is provided, comprising the steps of transmitting histotripsy therapy pulses into a target tissue with a histotripsy therapy transducer array having a plurality of transducer elements to generate cavitation in the target tissue, receiving acoustic cavitation emission signals from the cavitation with the histotripsy therapy transducer array, calculating a travel time from the cavitation to each transducer element of the ultrasound transducer array based on the received acoustic cavitation emission signals, and adjusting a transmission time delay for at least one of the plurality of transducer elements based on the calculated travel times such that subsequent histotripsy therapy pulses arrive at the target tissue simultaneously.

**[0034]** In some embodiments, calculating the travel time includes using information encoded in the acoustic cavitation emissions.

**[0035]** In one example, the information comprises a start time of the acoustic cavitation emission generated from cavitation expansion.

**[0036]** In some embodiments, the information comprises a start time of the acoustic cavitation emission generated from cavitation collapse.

**[0037]** In one embodiment, the information comprises a peak time from cavitation collapse.

**[0038]** A receive-drive circuit configured to be retrofitted onto one or more transducer elements of an existing transmit-only histotripsy system is provided, comprising a voltage divider configured to be electrically coupled to a first transducer element, the voltage divider configured to attenuate voltage signals received by the first transducer element, a diode-resistor voltage divider electrically coupled to the voltage divider, the diode-resistor voltage divider being configured to provide nonlinear attenuation to compress signals above a predetermined voltage, and being further configured to AC couple the received signals to an analog to digital converter.

**[0039]** In some embodiments, the voltage divider and the diode-resistor voltage divider are configured to be disposed on a first circuitry board and that is configured to be electrically

coupled to high-voltage histotripsy driving electronics disposed on a separate second circuitry board.

**[0040]** In another embodiment, the receive-drive circuit and high-voltage histotripsy driving electronics are disposed on a single circuitry board.

5 **[0041]** A transmit-receive histotripsy system is provided, comprising a transducer element, transmit electronics coupled to the transducer element and configured to deliver histotripsy pulses to the transducer element, a non-linear compressor receive electronics coupled to the transducer element, wherein the non-linear compressor receive electronics are configured to compress a first voltage signal with a first attenuation, and are further configured to compress a  
10 second voltage signal with a second attenuation, wherein the first voltage signal is higher than the second voltage signal and the first attenuation is higher than the second attenuation.

**[0042]** A transmit-receive driving electronics for a histotripsy system is also provided, comprising a transducer element, a secondary transformer coil electrically coupled to the transducer element, a primary transformer coil positioned adjacent to the secondary transformer  
15 coil, the primary transformer coil being configured to generate ultrasound pulses in the transducer element via the secondary transformer coil, a third transformer coil positioned adjacent to the secondary transformer coil, the third transformer coil being configured to attenuate voltage signals received by the transducer element by a predetermined amount.

**[0043]** In some embodiments, the third transformer coil is configured to attenuate the  
20 received voltage signals by 90-99%. In another embodiment, the third transformer coil is wound with approximately 7-10x fewer windings than the secondary transformer coil.

**[0044]** In some embodiments, the third transformer coil is configured to saturate during transmission of ultrasound pulses.

**[0045]** In another embodiment, the third transformer coil is coupled to a signal transformer  
25 with a specifically chosen core material and size such that the signal transformer is configured to saturate during transmission of ultrasound pulses.

**[0046]** A transmit-receive driving electronics of a histotripsy system is provided, comprising an ultrasound transducer array, transmission electronics coupled to the ultrasound transducer array and configured to transmit one or more histotripsy pulses to generate cavitation in a target  
30 tissue, receive electronics configured to receive acoustic cavitation emissions from the cavitation, a transmit-receive switch configured to enable only the transmission electronics during transmission of the one or more histotripsy pulses, the transmit-receive switch being further configured to enable only the receive electronics at a predetermined time after the

transmission of the one or more histotripsy pulses, to block transmission signals without attenuating received signals.

5 [0047] In one embodiment, a different linear gain follows the transmit-receive switch to amplify or attenuate a selected portion of the received signal based on its amplitude to maximize a receive sensitivity of the receive electronics.

10 [0048] A method histotripsy therapy is provided, comprising the steps of transmitting histotripsy therapy pulses into a target tissue with a histotripsy therapy transducer array to generate cavitation in the target tissue, receiving acoustic cavitation emission signals from the cavitation with the histotripsy therapy transducer, detecting a selected acoustic cavitation emission feature to separate from tissue signals, calculating a cavitation parameter that correlates to tissue damage generated by the histotripsy therapy pulses, determining a change in the cavitation parameter that correlates to treatment progression, determining a change in the cavitation parameter that correlates to treatment completion.

15 [0049] In one example, the selected acoustic cavitation emission feature comprises a timing of cavitation bubble expansion signals.

[0050] In another example, the selected acoustic cavitation emission feature comprises an amplitude of cavitation bubble expansion signals.

[0051] In some embodiments, the selected acoustic cavitation emission feature comprises a timing of cavitation bubble collapse signals.

20 [0052] In another embodiment, the selected acoustic cavitation emission feature comprises an amplitude of cavitation bubble collapse signals.

[0053] In some embodiments, the selected acoustic cavitation emission feature comprises a timing of cavitation bubble rebound signals.

25 [0054] In one embodiment, the selected acoustic cavitation emission feature comprises an amplitude of cavitation bubble rebound signals.

[0055] In another embodiment, the cavitation parameter comprises a collapse time of the cavitation.

[0056] In some examples, the collapse time comprises a time between expansion and collapse signals of the cavitation.

30 [0057] In another embodiment, the cavitation parameter comprises a peak amplitude of an expansion signal of the cavitation.

[0058] In some embodiments, the cavitation parameter comprises a peak amplitude of a collapse signal of the cavitation.

**[0059]** In another embodiment, the cavitation parameter comprises amplitude ratios of a growth ACE signal of the cavitation.

**[0060]** In some embodiments, the cavitation parameter comprises amplitude ratios of a collapse ACE signal of the cavitation.

5 **[0061]** In another embodiment, the cavitation parameter comprises a decay rate of rebound-associated ACE signal amplitudes.

**[0062]** In one example, determining a change in the cavitation parameter that correlates to treatment progression further comprises identifying an increasing slope in the cavitation parameter.

10 **[0063]** In another example, determining a change in the cavitation parameter that correlates to treatment completion further comprises identifying saturation of the change in the cavitation parameter.

**[0064]** A method for cavitation detection during histotripsy is provided, comprising the steps of transmitting histotripsy therapy pulses into a target tissue with a histotripsy therapy transducer array to generate cavitation in the target tissue, receiving acoustic cavitation emission signals from the cavitation with the histotripsy therapy transducer array, detecting a selected acoustic cavitation emission feature to separate from tissue signals, processing and forming a cavitation map based on the selected acoustic cavitation emission feature, and overlaying the cavitation map onto an image of the target tissue.

15  
20 **[0065]** In some examples, the selected acoustic cavitation emission feature comprises a timing of cavitation bubble expansion signals. In other examples, the selected acoustic cavitation emission feature comprises an amplitude of cavitation bubble expansion signals. In additional examples, the selected acoustic cavitation emission feature comprises a timing of cavitation bubble collapse signals. In one embodiment, the selected acoustic cavitation emission feature comprises an amplitude of cavitation bubble collapse signals. In some embodiments, the selected acoustic cavitation emission feature comprises a timing of cavitation bubble rebound signals. In another example, the selected acoustic cavitation emission feature comprises an amplitude of cavitation bubble rebound signals.

25  
30 **[0066]** A method of performing aberration correction during histotripsy therapy is provided, comprising the steps of transmitting histotripsy therapy pulses into a target tissue with a histotripsy therapy transducer array to generate cavitation in the target tissue, receiving acoustic cavitation emission signals from the cavitation with the histotripsy therapy transducer array, analyzing the acoustic cavitation emission signals to detect the cavitation generated in the target tissue, testing presets of transmission time delays to select a set of transmission time delays that

can maximize a peak signal amplitude in the detected cavitation, and applying the selected set of transmission time delays such that subsequent histotripsy therapy pulses arrive at the target tissue simultaneously.

5

## DETAILED DESCRIPTION

**[0067]** Provided herein are systems and methods that provide efficacious non-invasive and minimally invasive therapeutic, diagnostic and research procedures. In particular, provided herein are optimized systems and methods that provide targeted, efficacious histotripsy in a variety of different regions and under a variety of different conditions without causing undesired tissue damage to intervening/non-target tissues or structures.

10

**[0068]** Balancing desired tissue destruction in target regions with the avoidance of damage to non-target regions presents a technical challenge. This is particularly the case where time efficient procedures are desired. Conditions that provide fast, efficacious tissue destruction tend to cause undue heating in non-target tissues. Undue heating can be avoided by reducing energy or slower delivery of energy, both of which run contrary to the goals of providing a fast and efficacious destruction of target tissue. Provided herein are a number of technologies that individually and collectively allow for fast, efficacious target treatment without undesired damage to non-target regions.

15

**[0069]** The system, methods and devices of the disclosure may be used for the minimally or non-invasive acoustic cavitation and treatment of healthy, diseased and/or injured tissue, including in extracorporeal, percutaneous, endoscopic, laparoscopic, and/or as integrated into a robotically-enabled medical system and procedures. As will be described below, the histotripsy system may include various electrical, mechanical and software sub-systems, including a Cart, Therapy, Integrated Imaging, Robotics, Coupling and Software. The system also may comprise various Other Components, Ancillaries and Accessories, including but not limited to patient surfaces, tables or beds, computers, cables and connectors, networking devices, power supplies, displays, drawers/storage, doors, wheels, illumination and lighting and various simulation and training tools, etc. All systems, methods and means creating/controlling/delivering histotripsy are considered to be a part of this disclosure, including new related inventions disclosed herein.

25

**[0070]** In one embodiment, the histotripsy system is configured as a mobile therapy cart, which further includes a touchscreen display with an integrated control panel with a set of physical controls, a robotic arm, a therapy head positioned on the distal end of the robot, a patient coupling system and software to operate and control the system.

30

**[0071]** The mobile therapy cart architecture can comprise internal components, housed in a standard rack mount frame, including a histotripsy therapy generator, high voltage power supply, transformer, power distribution, robot controller, computer, router and modem, and an ultrasound imaging engine. The front system interface panel can comprise input/output locations for connectors, including those specifically for two ultrasound imaging probes (handheld and probe coaxially mounted in the therapy transducer), a histotripsy therapy transducer, AC power and circuit breaker switches, network connections and a foot pedal. The rear panel of the cart can comprise air inlet vents to direct airflow to air exhaust vents located in the side, top and bottom panels. The side panels of the cart include a holster and support mechanism for holding the handheld imaging probe. The base of the cart can be comprised of a cast base interfacing with the rack mounted electronics and providing an interface to the side panels and top cover. The base also includes four recessed casters with a single total locking mechanism. The top cover of the therapy cart can comprise the robot arm base and interface, and a circumferential handle that follows the contour of the cart body. The cart can have inner mounting features that allow technician access to cart components through access panels.

**[0072]** The touchscreen display and control panel may include user input features including physical controls in the form of six dials, a space mouse and touchpad, an indicator light bar, and an emergency stop, together configured to control imaging and therapy parameters, and the robot. The touchscreen support arm is configured to allow standing and seated positions, and adjustment of the touchscreen orientation and viewing angle. The support arm further can comprise a system level power button and USB and ethernet connectors.

**[0073]** The robotic arm can be mounted to the mobile therapy cart on arm base of sufficient height to allow reach and ease of use positioning the arm in various drive modes into the patient/procedure work space from set up, through the procedure, and take down. The robotic arm can comprise six degrees of freedom with six rotating joints, a reach of 850 mm and a maximum payload of 5 kg. The arm may be controlled through the histotripsy system software as well as a 12 inch touchscreen polyscope with a graphical user interface. The robot can comprise force sensing and a tool flange, with force (x, y, z) with a range of 50 N, precision of 3.5 N and accuracy of 4.0 N, and torque (x, y, z) with a range of 10.0 Nm, precision of 0.2 Nm and accuracy of 0.3 Nm. The robot has a pose repeatability of +/- 0.03mm and a typical TCP speed of 1 m/s (39.4 in/s). In one embodiment, the robot control box has multiple I/O ports, including 16 digital in, 16 digital out, 2 analog in, 2 analog out and 4 quadrature digital inputs, and an I/O power supply of 24V/2A. The control box communication comprises 500 Hz control frequency, Modbus TCP, PROFINET, ethernet/IP and USB 2.0 and 3.0.

**[0074]** The therapy head can comprise one of a select group of four histotripsy therapy transducers and an ultrasound imaging system/probe, coaxially located in the therapy transducer, with an encoded mechanism to rotate said imaging probe independent of the therapy transducer to known positions, and a handle to allow gross and fine positioning of the therapy head, including user inputs for activating the robot (e.g. for free drive positioning). In some examples, the therapy transducers may vary in size (22 x 17 cm to 28 x 17 cm), focal lengths from 12 – 18 cm, number of elements, ranging from 48 to 64 elements, comprised within 12-16 rings, and all with a frequency of 700 kHz. The therapy head subsystem has an interface to the robotic arm includes a quick release mechanism to allow removing and/or changing the therapy head to allow cleaning, replacement and/or selection of an alternative therapy transducer design (e.g., of different number of elements and geometry), and each therapy transducer is electronically keyed for auto-identification in the system software.

**[0075]** The patient coupling system can comprise a six degree of freedom, six joint, mechanical arm, configured with a mounting bracket designed to interface to a surgical/interventional table rail. The arm may have a maximum reach of approximately 850 mm and an average diameter of 50 mm. The distal end of the arm can be configured to interface with an ultrasound medium container, including a frame system and an upper and lower boot. The lower boot is configured to support either a patient contacting film, sealed to patient, or an elastic polymer membrane, both designed to contain ultrasound medium (e.g., degassed water or water mixture), either within the frame and boot and in direct contact with the patient, or within the membrane/boot construct. The lower boot provides, in one example, a top and bottom window of approximately 46 cm x 56 cm and 26 cm x 20 cm, respectively, for placing the therapy transducer with the ultrasound medium container and localized on the patient's abdomen. The upper boot may be configured to allow the distal end of the robot to interface to the therapy head and/or transducer, and to prevent water leakage/spillage. In preferred embodiments, the upper boot is a sealed system. The frame is also configured, in a sealed system, to allow two-way fluid communication between the ultrasound medium container and an ultrasound medium source (e.g., reservoir or fluidics management system), including, but not limited to filling and draining, as well as air venting for bubble management.

**[0076]** The system software and workflow can be configured to allow users to control the system through touchscreen display and the physical controls, including but not limited to, ultrasound imaging parameters and therapy parameters. The graphical user interface of the system comprises a workflow based flow, with the general procedure steps of 1) registering/selecting a patient, 2) planning, comprising imaging the patient (and target

location/anatomy) with the freehand imaging probe, and robot assisted imaging with the transducer head for final gross and fine targeting, including contouring the target with a target and margin contour, of which are typically spherical and ellipsoidal in nature, and running a test protocol (e.g., test pulses) including a bubble cloud calibration step, and a series of

5 predetermined locations in the volume to assess cavitation initiation threshold and other patient/target specific parameters (e.g., treatment depth), that together inform a treatment plan accounting for said target's location and acoustic pathway, and any related blockage (e.g., tissue interfaces, bone, etc.) that may require varied levels of drive amplitude to initiate and maintain histotripsy. Said parameters, as measured as a part of the test protocol, comprising calibration

10 and multi-location test pulses, are configured in the system to provide input/feedback for updating bubble cloud location in space as needed/desired (e.g., appropriately calibrated to target cross-hairs), as well as determining/interpolating required amplitudes across all bubble cloud treatment locations in the treatment volume to ensure threshold is achieved throughout the volume. Further, said parameters, including but not limited to depth and drive voltage, may be

15 also used as part of an embedded treatability matrix or look up table to determine if additional cooling is required (e.g., off-time in addition to time allocated to robot motions between treatment pattern movements) to ensure robust cavitation and intervening/collateral thermal effects are managed (e.g., staying below t43 curve for any known or calculated combination of sequence, pattern and pathway, and target depth/blockage). The workflow and procedure steps

20 associated with these facets of planning, as implemented in the system software may be automated, wherein the robot and controls system are configured to run through the test protocol and locations autonomously, or semi-autonomously. Following planning, the next phase of the procedure workflow, 3) the treatment phase, is initiated following the user accepting the treatment plan and initiating the system for treatment. Following this command, the system is

25 configured to deliver treatment autonomously, running the treatment protocol, until the prescribed volumetric treatment is complete. The status of the treatment (and location of the bubble cloud) is displayed in real-time, adjacent to various treatment parameters, including, but not limited to, of which may include total treatment time and remaining treatment time, drive voltage, treatment contours (target/margin) and bubble cloud/point locations, current location in

30 treatment pattern (e.g., slice and column), imaging parameters, and other additional contextual data (e.g., optional DICOM data, force torque data from robot, etc.). Following treatment, the user may use the therapy head probe, and subsequently, the freehand ultrasound probe to review and verify treatment, as controlled/viewed through the system user interface. If additional target

locations are desired, the user may plan/treat additional targets, or dock the robot to a home position on the cart if no further treatments are planned.

[0077] FIG. 1A generally illustrates histotripsy system 100 according to the present disclosure, comprising a therapy transducer 102, an imaging system 104, a display and control panel 106, a robotic positioning arm 108, and a cart 110. The system can further include an ultrasound coupling interface and a source of coupling medium, not shown.

[0078] FIG. 1B is a bottom view of the therapy transducer 102 and the imaging system 104. As shown, the imaging system can be positioned in the center of the therapy transducer. However, other embodiments can include the imaging system positioned in other locations within the therapy transducer, or even directly integrated into the therapy transducer. In some embodiments, the imaging system is configured to produce real-time imaging at a focal point of the therapy transducer.

[0079] The histotripsy system may comprise one or more of various sub-systems, including a Therapy sub-system that can create, apply, focus and deliver acoustic cavitation/histotripsy through one or more therapy transducers, Integrated Imaging sub-system (or connectivity to) allowing real-time visualization of the treatment site and histotripsy effect through-out the procedure, a Robotics positioning sub-system to mechanically and/or electronically steer the therapy transducer, further enabled to connect/support or interact with a Coupling sub-system to allow acoustic coupling between the therapy transducer and the patient, and Software to communicate, control and interface with the system and computer-based control systems (and other external systems) and various Other Components, Ancillaries and Accessories, including one or more user interfaces and displays, and related guided workflows, all working in part or together. The system may further comprise various fluidics and fluid management components, including but not limited to, pumps, valve and flow controls, temperature and degassing controls, and irrigation and aspiration capabilities, as well as providing and storing fluids. It may also contain various power supplies and protectors.

## **CART**

[0080] The Cart 110 may be generally configured in a variety of ways and form factors based on the specific uses and procedures. In some cases, systems may comprise multiple Carts, configured with similar or different arrangements. In some embodiments, the cart may be configured and arranged to be used in a radiology environment and in some cases in concert with imaging (e.g., CT, cone beam CT and/or MRI scanning). In other embodiments, it may be arranged for use in an operating room and a sterile environment, or in a robotically enabled operating room, and used alone, or as part of a surgical robotics procedure wherein a surgical

robot conducts specific tasks before, during or after use of the system and delivery of acoustic cavitation/histotripsy. As such and depending on the procedure environment based on the aforementioned embodiments, the cart may be positioned to provide sufficient work-space and access to various anatomical locations on the patient (e.g., torso, abdomen, flank, head and neck, etc.), as well as providing work-space for other systems (e.g., anesthesia cart, laparoscopic tower, surgical robot, endoscope tower, etc.).

**[0081]** The Cart may also work with a patient surface (e.g., table or bed) to allow the patient to be presented and repositioned in a plethora of positions, angles and orientations, including allowing changes to such to be made pre, peri and post-procedurally. It may further comprise the ability to interface and communicate with one or more external imaging or image data management and communication systems, not limited to ultrasound, CT, fluoroscopy, cone beam CT, PET, PET/CT, MRI, optical, ultrasound, and image fusion and or image flow, of one or more modalities, to support the procedures and/or environments of use, including physical/mechanical interoperability (e.g., compatible within cone beam CT work-space for collecting imaging data pre-, peri- and/or post-histotripsy).

**[0082]** In some embodiments one or more Carts may be configured to work together. As an example, one Cart may comprise a bedside mobile Cart equipped with one or more Robotic arms enabled with a Therapy transducer, and Therapy generator/amplifier, etc., while a companion cart working in concert and at a distance of the patient may comprise Integrated Imaging and a console/display for controlling the Robotic and Therapy facets, analogous to a surgical robot and master/slave configurations.

**[0083]** In some embodiments, the system may comprise a plurality of Carts, all slave to one master Cart, equipped to conduct acoustic cavitation procedures. In some arrangements and cases, one Cart configuration may allow for storage of specific sub-systems at a distance reducing operating room clutter, while another in concert Cart may comprise essentially bedside sub-systems and componentry (e.g., delivery system and therapy).

**[0084]** One can envision a plethora of permutations and configurations of Cart design, and these examples are in no way limiting the scope of the disclosure.

## **HISTOTRIPSY**

**[0085]** Histotripsy comprises short, high amplitude, focused ultrasound pulses to generate a dense, energetic, “bubble cloud”, capable of the targeted fractionation and destruction of tissue. Histotripsy is capable of creating controlled tissue erosion when directed at a tissue interface, including tissue/fluid interfaces, as well as well-demarcated tissue fractionation and destruction, at sub-cellular levels, when it is targeted at bulk tissue. Unlike other forms of ablation, including

thermal and radiation-based modalities, histotripsy does not rely on heat or ionizing (high) energy to treat tissue. Instead, histotripsy uses acoustic cavitation generated at the focus to mechanically effect tissue structure, and in some cases liquefy, suspend, solubilize and/or destruct tissue into sub-cellular components.

5 **[0086]** Histotripsy can be applied in various forms, including: 1) Intrinsic-Threshold Histotripsy: Delivers pulses with at least a single negative/tensile phase sufficient to cause a cluster of bubble nuclei intrinsic to the medium to undergo inertial cavitation, 2) Shock-Scattering Histotripsy: Delivers typically pulses 3-20 cycles in duration. The amplitude of the tensile phases of the pulses is sufficient to cause bubble nuclei in the medium to undergo inertial  
10 cavitation within the focal zone throughout the duration of the pulse. These nuclei scatter the incident shockwaves, which invert and constructively interfere with the incident wave to exceed the threshold for intrinsic nucleation, and 3) Boiling Histotripsy: Employs pulses roughly 1-20 ms in duration. Absorption of the shocked pulse rapidly heats the medium, thereby reducing the threshold for intrinsic nuclei. Once this intrinsic threshold coincides with the peak  
15 negative pressure of the incident wave, boiling bubbles form at the focus.

**[0087]** The large pressure generated at the focus causes a cloud of acoustic cavitation bubbles to form above certain thresholds, which creates localized stress and strain in the tissue and mechanical breakdown without significant heat deposition. At pressure levels where cavitation is not generated, minimal effect is observed on the tissue at the focus. This cavitation  
20 effect is observed only at pressure levels significantly greater than those which define the inertial cavitation threshold in water for similar pulse durations, on the order of 10 to 30 MPa peak negative pressure.

**[0088]** Histotripsy may be performed in multiple ways and under different parameters. It may be performed totally non-invasively by acoustically coupling a focused ultrasound  
25 transducer over the skin of a patient and transmitting acoustic pulses transcutaneously through overlying (and intervening) tissue to the focal zone (treatment zone and site). It may be further targeted, planned, directed and observed under direct visualization, via ultrasound imaging, given the bubble clouds generated by histotripsy may be visible as highly dynamic, echogenic regions on, for example, B Mode ultrasound images, allowing continuous visualization through  
30 its use (and related procedures). Likewise, the treated and fractionated tissue shows a dynamic change in echogenicity (typically a reduction), which can be used to evaluate, plan, observe and monitor treatment.

**[0089]** Generally, in histotripsy treatments, ultrasound pulses with 3 or more acoustic cycles are applied, and the bubble cloud formation relies on the pressure release scattering of the

positive shock fronts (sometimes exceeding 100 MPa, P+) from initially initiated, sparsely distributed bubbles (or a single bubble). This is referred to as the “shock scattering mechanism”.

5 [0090] This mechanism depends on one (or a few sparsely distributed) bubble(s) initiated with the initial negative half cycle(s) of the pulse at the focus of the transducer. A cloud of microbubbles then forms due to the pressure release backscattering of the high peak positive shock fronts from these sparsely initiated bubbles. These back-scattered high-amplitude rarefactional waves exceed the intrinsic threshold thus producing a localized dense bubble cloud. Each of the following acoustic cycles then induces further cavitation by the backscattering from the bubble cloud surface, which grows towards the transducer. As a result, an elongated dense bubble cloud growing along the acoustic axis opposite the ultrasound propagation direction is observed with the shock scattering mechanism. This shock scattering process makes the bubble cloud generation not only dependent on the peak negative pressure, but also the number of acoustic cycles and the amplitudes of the positive shocks. Without at least one intense shock front developed by nonlinear propagation, no dense bubble clouds are generated when the peak negative half-cycles are below the intrinsic threshold.

15 [0091] When ultrasound pulses less than 2 cycles are applied, shock scattering can be minimized, and the generation of a dense bubble cloud depends on the negative half cycle(s) of the applied ultrasound pulses exceeding an “intrinsic threshold” of the medium. This is referred to as the “intrinsic threshold mechanism”.

20 [0092] This threshold can be in the range of 26 – 30 MPa for soft tissues with high water content, such as tissues in the human body. In some embodiments, using this intrinsic threshold mechanism, the spatial extent of the lesion may be well-defined and more predictable. With peak negative pressures (P-) not significantly higher than this threshold, sub-wavelength reproducible lesions as small as half of the -6dB beam width of a transducer may be generated.

25 [0093] With high-frequency Histotripsy pulses, the size of the smallest reproducible lesion becomes smaller, which is beneficial in applications that require precise lesion generation. However, high-frequency pulses are more susceptible to attenuation and aberration, rendering problematical treatments at a larger penetration depth (e.g., ablation deep in the body) or through a highly aberrative medium (e.g., transcranial procedures, or procedures in which the pulses are transmitted through bone(s)). Histotripsy may further also be applied as a low-frequency “pump” pulse (typically < 2 cycles and having a frequency between 100 kHz and 1 MHz) can be applied together with a high-frequency “probe” pulse (typically < 2 cycles and having a frequency greater than 2 MHz, or ranging between 2 MHz and 10 MHz) wherein the peak negative pressures of the low and high-frequency pulses constructively interfere to exceed the

intrinsic threshold in the target tissue or medium. The low-frequency pulse, which is more resistant to attenuation and aberration, can raise the peak negative pressure  $P_-$  level for a region of interest (ROI), while the high-frequency pulse, which provides more precision, can pinpoint a targeted location within the ROI and raise the peak negative pressure  $P_-$  above the intrinsic threshold. This approach may be referred to as “dual frequency”, “dual beam histotripsy” or “parametric histotripsy.”

**[0094]** Additional systems, methods and parameters to deliver optimized histotripsy, using shock scattering, intrinsic threshold, and various parameters enabling frequency compounding and bubble manipulation, are herein included as part of the system and methods disclosed herein, including additional means of controlling said histotripsy effect as pertains to steering and positioning the focus, and concurrently managing tissue effects (e.g., prefocal thermal collateral damage) at the treatment site or within intervening tissue. Further, it is disclosed that the various systems and methods, which may include a plurality of parameters, such as but not limited to, frequency, operating frequency, center frequency, pulse repetition frequency, pulses, bursts, number of pulses, cycles, length of pulses, amplitude of pulses, pulse period, delays, burst repetition frequency, sets of the former, loops of multiple sets, loops of multiple and/or different sets, sets of loops, and various combinations or permutations of, etc., are included as a part of this disclosure, including future envisioned embodiments of such.

#### **TECHNICAL CHALLENGES WITH HISTOTRIPSY**

**[0095]** There are two technical challenges for using ultrasound therapy such as histotripsy to treat a deep tissue target (e.g., >8 cm) or through heterogenous tissue: 1) acoustic aberration and 2) real-time feedback of the ultrasound therapy.

**[0096]** Acoustic aberration is a problem that impacts ultrasound therapy and imaging, including histotripsy. Acoustic aberration can reduce the focal pressure and distort the focus due to ultrasound propagation through multi-layer heterogenous tissue. Reduction of the focal pressure can cause ineffective treatment or reduced treatment efficiency. For example, in histotripsy, focal pressures at the target tissue site are precisely controlled to generate cavitation at the target tissue site. Reduction of the focal pressures due to aberration can prevent cavitation from occurring. Distortion of the focus can also decrease treatment accuracy. Typically, a focused ultrasound transducer is shaped as a segment of a spherical surface, such that the sound wave emitted from all locations from the transducer surface go through the same distance to arrive at the focus at the same time. However, due to the variation of speed of sound across bones and heterogeneous soft tissue, the travel time from different elements of an ultrasound

transducer array to arrive at the focus may be different. As a result, aberration can result in loss of focal pressure and defocusing, decreasing treatment efficacy and accuracy.

**[0097]** As ultrasound is a non-invasive therapy technique, real-time feedback is critical to achieve high treatment accuracy and minimizing any potential complications. Ultrasound  
5 imaging has been used to provide real-time feedback for histotripsy, as histotripsy-generated cavitation can be visualized on ultrasound images as a dynamic, bright zone. Typically, an ultrasound imaging probe is inserted in a central hole of the histotripsy transducer, thus the 2D ultrasound imaging plane contains the histotripsy focus. Ultrasound imaging can then be used to guide the targeting to place histotripsy focus to the correct target tissue and to monitor the  
10 treatment progression. However, there are two main limitations of using ultrasound imaging as the sole guidance for histotripsy. 1) When the ultrasound imaging probe is blocked by bone of the patient (e.g., ribs or skull), ultrasound images of the histotripsy focus cannot be obtained. For example, histotripsy can be used to treat a tumor volume in the liver of a patient, which is partially behind the ribcage. When the histotripsy transducer is mechanically moved to scan the  
15 histotripsy focus to cover the tumor volume, the imaging probe can be blocked by the ribs for a certain duration of the therapy, at which point no real-time imaging of the therapy is available due to the rib blockage. Without any feedback during this duration, there is no way of knowing if cavitation is still generated at the target locations in the tumor (i.e., if the treatment is implemented over this duration). 2) Ultrasound imaging probes can only view the tissue and  
20 cavitation within the 2D image plane that contains the histotripsy focus. Thus, ultrasound imaging probes cannot view any potential unwanted cavitation occurring outside the image plane. Unwanted cavitation may generate undesired off-target damage.

**[0098]** The problems described above can be solved with a novel histotripsy ultrasound phased array transducer, as described herein, that is configured to transmit ultrasound signals to  
25 generate cavitation and deliver histotripsy as well as is configured to receive ultrasound signals (i.e., a transmit-receive histotripsy array).

**[0099]** For example, when the ultrasound therapy transducer comprises a phased array, phase correction techniques can be used to correct aberration to recover reduced focal pressure. This can be accomplished by adjusting the phase/time delay at transmission from each transducer  
30 element of the phased array to compensate for the travel time variation from each array element to the focus due to the speed of sound variation. In doing so, the aberration can be corrected to increase the focal pressure and improve the focusing.

**[0100]** An ultrasound phased array transducer that can delivery histotripsy and receive acoustic cavitation emission signals can further be configured to allow detection, localization,

and mapping of cavitation. Currently, a typical histotripsy system only transmits ultrasound pulses to generate cavitation at the focus. A transmit-receive histotripsy system can not only be used to deliver ultrasound pulses to generate cavitation, but also can receive signals such as the acoustic cavitation emission (ACE) signals. Both the rapid expansion and rapid collapse of cavitating bubbles during histotripsy produce shockwaves that can be detected by an acoustic receiver. In some embodiments, received reflections of the main therapy pulse (if > 1-2 cycles long and not fully transformed to shockwave in cavitation generation event) or subsequent low amplitude therapy pulses could be used in various receive application listed below. By processing the ACE signals received from a histotripsy transducer array system with hundreds of elements and transmit-receive capability, cavitation can be detected and localized to provide a real-time, 3D cavitation map. The acoustic emission signals from the growth and/or collapse of histotripsy-induced cavitation microbubbles, received by the histotripsy array, can be used to localize and monitor the cavitation in 3D and real-time, even in situations where the ultrasound imaging probe is blocked by bone. 3D cavitation mapping can also allow real-time monitoring of any off-focus cavitation to increase safety and identify unwanted cavitation.

**[0101]** Transmit-receive driving electronics found in typical phased array systems cannot be directly adapted for a histotripsy phased array transducer because of the extremely high voltages (thousands of volts) necessary for generating high-pressure histotripsy pulses. A novel driving electronics, as described herein, is configured to safely block or significantly attenuate the transmit signal to the ultrasound transducer array while maintaining high sensitivity and high dynamic range for received ultrasound signals. This disclosure provides both hardware and software for a phased array histotripsy transducer array with transmit and receive capability. This disclosure further describes the methods and signal processing algorithms that can be used with the transmit-receive histotripsy system for aberration correction and cavitation mapping.

## **TRANSMIT-RECEIVE ELECTRIC DRIVING SYSTEM**

**[0102]** The electric transmit signal to a histotripsy transducer is typically on the order of Kilovolts, while received ultrasound signals typically range from millivolts to tens of Volts. Thus, the transmit-receive electric driving circuitry as described herein is designed and configured to block or heavily attenuate the high-amplitude transmit waveform signals on the order of thousands of Volts, while having sufficient sensitivity and dynamic range to receive the low-amplitude signals on the order of tens of Volts.

**[0103]** Many drive circuitry embodiments and implementations to achieve the stated function/purpose above are described herein. In some examples, the drive circuitry can be retrofitted or added-on to an existing transmit-only histotripsy system to provide transmit-receive

capabilities. In other embodiments, the drive circuitry is integrated into an entirely new transmit-receive histotripsy system.

**[0104]** FIG. 2A is one embodiment of a novel receive drive circuitry 200 configured to be retrofitted onto an existing transmit-only histotripsy system to enable transmit-receive functionality. In the illustrated schematic drawing, a non-linear compressor can attenuate all the signals connected to each of the histotripsy elements, but with more attenuation for the high-amplitude signals and less attenuation for the low-amplitude signals. For example, a capacitive voltage divider 202, as indicated by C1 and C2, can first be configured to attenuate all incoming/received voltage signals from transducer element TX1 to approximately 1-10% (or to attenuate the signals by 90-99%). Then a diode-resistor voltage divider 204, as indicated by D1, D2, and C3, is configured to provide nonlinear attenuation to compress all signals above approximately 1 Volts and alternating current (AC) couple the signal into the analog to digital converter (ADC) for ADC conversion. The final component before the ADC is a voltage level shifter 206, as indicated by R2 and R3, that puts the signal in the appropriate voltage range for the ADC (e.g., typically between +/- 0.5V to +/- 2V). As described above, this circuitry is configured to be retrofitted to an existing transmit-only histotripsy driving system. For example, separate circuitry boards can be added and connected to the existing transmit circuitry to add the receive functions. In one embodiment, the receive circuitry is added in parallel to the transmit electronics and passively receives signals without affecting the transmit electronics.

**[0105]** FIG. 2B is one embodiment of a drive circuitry 200a that is integrated into high voltage histotripsy driving electronics. In the embodiment of FIG. 2B, a bank of capacitors (not shown) in series with the primary coil 20 of the transformer are charged by a high voltage supply. A driver chip, U1, then triggers the n-channel MOSFET transistor, Q1, which sends a high voltage AC pulse through the transformer primary coil thereby generating an AC pulse in the transformer secondary coil 22 with a voltage proportional to the turn ratio between the coils. The secondary coil can be electrically coupled to each of the transducer elements (in this illustration, transducer element TX1). In one implementation, a turn ratio of approximately 1:3 was used between the primary and secondary coils. This receive drive circuitry is thereby able to generate single-cycle pulses at the center frequency of the transducer on the order of 3 kV. It should be understood that other turn ratios can be implemented.

**[0106]** Referring to FIG. 2C, another embodiment of receive drive electronics for a histotripsy system are shown. As shown, the receive drive electronics can include a secondary transformer coil 22 coupled to the transducer element TX1. Because the driver for this system already includes a transformer at the output of each channel, a third coil 24 can be added to each

transformer to be used for the receive electronics, thereby providing total isolation between the driver (e.g., the primary coil 20) and the receiver (e.g., third coil 24). In one implementation, the receive or third coil can be wound with approximately 10-times fewer windings than the secondary transformer coil 22, thereby providing a 10X reduction in voltage between the secondary coil and the third coil. The number of windings on the tertiary or third coil can be tuned for the specific application and need not necessarily be 10-times fewer than the secondary. The ratio depends on the receive signal amplitude and can be adjusted based on desired voltages. In one embodiment, the receive winding (third coil 24) from Fig. 2C can be coupled to a second transformer designed for small signal use with the specifically chosen core material and size such that it would be configured to saturate during the transmit pulses to protect the analog to digital circuitry (ADC) behind it. When receiving signals, however, the second small signal transformer would be configured to not saturate, thereby enabling the appropriate gain and sensitivity for the received signals.

**[0107]** A schematic design of receive circuitry for the integrated receive-capable histotripsy system is shown in FIG. 2D. The primary difference in the embodiment shown in FIG. 2D compared to the embodiment above in FIG. 2A is the transformer, which is described in the embodiment of FIG. 2C. The VGA circuit is added in the embodiment of FIG. 2D, and the “balanced” input with the two capacitors C3 and C4 in series instead of the level shifter as shown in FIG. 2A comprises a digitizer.

**[0108]** In another embodiment, the transmit-receive drive circuitry can include a transmit-receive switch. An integrated drive-receive circuitry with both transmit and receive circuitry on the same board can use a switch to separate the receive signal from the transmit signal. For example, a traditional TR switch with diodes blocks high-voltage transmit signals without attenuating receive signals. A circuit with different linear gain can follow the switch to amplify or attenuate the selected portion of the receive signal properly based on its amplitude to maximize the sensitivity. However, this design would waste a lot of power, be large, and expensive.

**[0109]** FIG. 3A illustrates another embodiment of drive-receive circuitry that is configured to measure current flowing back from the transducer TX1 through the drive transformer T1 (instead of measuring voltage generated on the transducer during receive as discussed above). The relatively large surface area of therapy transducer array elements compared to a traditional imaging transducer means the transducer array generates a relatively large current, which makes high sensitivity during receive possible, whereas with an imaging transducer, it is only practical to measure the voltage induced by acoustic signals. Normal ultrasound imaging elements would

be too small to generate a useable receive current. Therapy elements as described herein are hundreds to thousands of times larger in surface area than traditional imaging elements, so the currents are substantially larger and easy to measure (in the milliamp range rather than microamp). In the circuitry illustrated, current can be measured by a sense resistor in the electrical path (R1). The drive-receive circuitry is configured to pass excess current from large reflections or during the transmit pulse through a set of bypass diodes (D1 and D2). Transmit currents can be as large as 40 A. While the drive-receive circuitry is receiving reflections such as ultrasound reflection signals and/or acoustic cavitation emissions, the sense resistor is configured to measure a current induced in the circuitry by those reflections. Voltage generated across the current sensing resistor is coupled to the ADC through a Balun (T2) and Capacitors C1 and C2. This balanced input configuration is the manufacturer's preferred circuit for the AFE5801 digitizer. Single-ended operation would also be possible for this or other digitizers by directly measuring the voltage on R1 with respect to ground.

**[0110]** The drive-receive circuitry of FIG. 3A can be configured to operate in a low gain mode and a high gain mode. Referring still to FIG. 3A, the circuitry can have two current sensing resistors R1 and R2 so that the overall sensitivity of the circuit can be changed by a large amount. As shown, this can be implemented with a pair of transistors Q2 and Q3 that are configured to switch on/off a small value resistor R2 (low sensitivity) in parallel with the larger value resistor R1 (high sensitivity). The resistance of the circuit can be changed very rapidly with these transistors to enable the use of both the low setting over part of a received burst of data (e.g., a received signal with a higher amplitude such as ultrasound reflection signals from bones) and the high setting a few microseconds later (e.g., a received signal with a lower amplitude such as acoustic cavitation emission signal from cavitation collapse). Because the sensor is directly changed, both scales have very high SNR unlike a variable gain amplifier where the SNR is usually worse for higher gain. In some embodiments, additional sense resistors can be implemented in the same manner for even wider dynamic range. For the circuit shown in FIG. 3A, the high gain mode is configured to measure currents up to 5 mA in the ADC which is coupled to the circuitry via transformer T2, while the low gain mode is configured to measure currents up to 200 mA in the ADC.

**[0111]** FIG. 3B shows an alternate embodiment where instead of bypass diodes, low gate threshold MOSFET transistors Q4 and Q5 can be implemented for passing the large transmit currents. With the advances in transistors, there are now transistors that are smaller, cheaper, and higher performance than any diode for this bypass role. These transistors can have a higher

turn on voltage than a single diode, which allows the use of the full dynamic range of the ADC more easily.

**[0112]** FIG. 3C shows a third embodiment where the bypass transistors Q4 and Q5 are explicitly controlled as an active transmit-receive switch. The transistor gates are connected to a gate drive signal to force the transistors fully on (for transmit mode) or fully off (for receive mode) which could be +/- 5 V, for example, depending on the transistor drive requirements. This configuration may reduce RF noise generated during transmit where instead passively switched bypass components must turn on and off rapidly at the frequency of the ultrasound. This design has a tradeoff of a minor increase in complexity.

**[0113]** The analog received signals described above can be converted to digital signals and then collected and processed. The signal received from the histotripsy transducer array can be, for example, reflections from bones or soft tissue or acoustic emission signals from cavitation. These signals are typically received in a specific time window after the histotripsy pulse (e.g., tens to hundreds of microseconds after transmission of the therapy pulse(s)). Thus, the hardware and software described herein is configured to synchronize the time clock of transmit, receive, and ADC conversion and sampling to obtain the appropriate time window after each histotripsy pulse that contains the desired received signals. If the synchronization and time window is set properly, then the desired received signals can be collected and processed.

**[0114]** To achieve proper synchronization and time windowing, any of the transmit-receive drive electronics described herein can include an embodiment in which a single field-programmable gated array (FPGA) device connected to the ADC can be used to control both the transmit and receive operations of the transducer, as well as the ADC for some subset of or all channels of a histotripsy system. By providing the FPGA with a single clock off of which the timings of the operations to be executed by the separate subsystems are based, synchronization between subsystems can be guaranteed especially when multiple FPGAs are used to control various subsets of histotripsy transducer elements. Setting the appropriate time window to receive the signals can then be achieved through appropriate assignment of the timings of the respective operations when programming of the FPGA. In cases where multiple FPGAs are required, for instance in arrays with too many transducer elements to control from a single device, a single clock line can be fanned out to all of them for synchronization, and a centralized 'master' FPGA can be used to trigger the execution of their operations within the appropriate time window.

**[0115]** Alternatively, any of the transmit-receive driving electronics described herein can include multi-FPGA systems can be setup to run in a 'headless' mode wherein no centralized

'master' FPGA is required to issue/fan out a single shared clock line or trigger the execution of individual boards' operations. In such a mode, each FPGA would be set to run off of its own individual clock and to monitor and update two common 'program-execution-state', and one common 'execute-operation', open-drain hardware IO lines shared by the whole system. The open-drain lines operate such that, if any single FPGA applies a low signal to the lines, the signal measured anywhere on the line would register low; if and only if all FPGAs apply a high signal to the lines, the signal measured everywhere on the line would register high. The two 'program-execution-state' lines would be used to the FPGAs to issue system-wide 1) 'ready-to-execute' and 2) 'done-executing' signals and by default each FPGA would apply a low signal to each of these lines; each FPGA would apply a high signal to the 'execute-operation' line. While running a program, upon reaching a new executable instruction in the program, each FPGA would update the 'ready-to-execute' line to apply a high signal to it, and enter a wait state wherein it would monitor the signals on both the 'ready-to-execute' line and the 'execute-operation' lines. Once all FPGAs reached the 'ready-to-execute' state, the signal registered on the 'ready-to-execute' line would become high; the first FPGA in the system to detect a high state on the 'ready-to-execute' line would issue a low signal on the 'execute-program' line causing it to register low everywhere. Upon detection of the low signal on the 'execute-program' line, each FPGA would set the value on its own terminal of the 'execute-program' line to be low and execute its stored commands. Once each FPGA finished running its respective commands, it would apply a high signal to both the 'done-executing' and 'execute-program' lines. Once both the 'done-executing' and 'execute-program' lines registered high, the FPGAs would reset all of the shared open-drain line values to their defaults, load the next instruction in the program, and repeat the process for each instruction until the program was completed.

**[0116]** A fully connected set of receiving elements can generate large amounts of data, so strategies to reduce the data load are proposed to allow acquired signals to be transferred and processed in real-time to meet the monitoring needs during therapy. These strategies can be applied to any of the transmit-receive driving electronics described herein. Such strategies may include, for example, artificially down sampling the incoming data from the ADC in the firmware running on FPGA (e.g., by storing only every other data point generated by the ADC, or the average of the data points generated across multiple acquisition cycles). This effectively reduces the sampling frequency, thus reducing the data load, but doesn't sacrifice temporal precision or dynamic range or result in an increase in noise in the system. Differential compression schemes, wherein all data captured after the first time point is stored as the difference between the values captured at adjacent time points may also be applied. For

example, for a value at time 1 of X, and at time 2 of Y, one could store the value of the difference between Y and X,  $D = Y - X$ , at time 2 instead of the value of Y directly, and then calculate the actual value of Y during processing as  $Y = X + D$ . In this way, nominal values of say  $X=64000$  and  $Y=63900$ , which combined represent 4 bytes of data, could be stored as  
5  $X=64000$  and  $D=-100$ , which combined represent 3 bytes of data and allow the full recovery of the value of Y. As the length of the data record gets longer, this compression strategy results in data reductions proportional to ratio of the size of the variable needed to store the difference value compared to the size of the variable required to store the actual value, which can generally reduce data loads in the current system by 30%-50%, but could result in significantly larger  
10 reductions in systems where the individual data elements are larger in size. In applications not demanding real-time processing/compression, further reductions in data size can be achieved through frequency domain transforms using methods similar to those employed to compress audio files.

**[0117]** As some of the events that need to be monitored during histotripsy therapies will require very high temporal precision (e.g., the signals from individual cavitation events), while others will require little precision (e.g., the reflections of signals off of large boundaries, e.g., the skull, ribs, tissue interfaces), strategies to dynamically alter the compression ratio can be implemented to fully utilize the incoming data for real-time applications. To that end, the firmware and software that control the data acquisition have been configured such that the  
15 sampling frequency and compression strategy used during acquisition can be set on a per-channel basis in the array, and can be independently updated in real-time, even in the middle of an individual acquisition event. This allows for different sub-apertures of the array to be set up to monitor different features of the therapy at the requisite sampling frequency and compression settings, as well as for the receive system to be set to the maximum sampling  
20 frequency/minimum compression settings across all elements of the array as needed to monitor short-lived events with potentially weak signals, and then set back to lower sampling frequencies with higher compression settings outside the window requiring maximal monitoring. This allows short-lived events of this type to be fully monitored without necessitating cut-offs in the acquisition to reduce the data load which could otherwise potentially result in reducing the  
25 physical size of the actively-monitored field or drastic reductions in monitoring speed during therapy.

**[0118]** In some situations, the receive signal amplitude may be low and the noise may be high, resulting in a low signal-to-noise ratio (SNR). One method to reduce the noise and increase SNR is to oversample and average in firmware (e.g., FPGA firmware) before storing  
30

data. This also helps increase dynamic range and reduces memory requirements. Another technique is to implement a dynamic variable sample rate. For example, the ADC can be configured to always run at 50 MHz, but high time precision may only be needed over certain portions of the data record. In the portions of the signals where such a high frame rate is not  
5 needed, samples can be decimated or averaged to greatly reduce storage requirements.

**[0119]** The bandwidth of the therapy transducer elements is typically low, but a high sampling rate can be used for sampling for good timing precision. Receive data should compress exceptionally well in the Fourier domain (at least a factor of 10, maybe a lot more). The FPGAs can be configured to perform this compression before storage or transmit either in firmware or in  
10 software. Data compression is the key to implementing real time monitoring, the system will be overwhelmed by the amount of receive data collected.

**[0120]** In applications where real time monitoring is not essential, or where treatment speed needs to remain higher than possible while simultaneously transferring the full acquired signals to the user's computer after each pulse, the system can be configured to transfer only partial  
15 signals and/or store the acquired signals directly on the FPGA devices themselves for transfer to the control computer later. This would allow uninterrupted acquisition of signals from all delivered pulses without limiting treatment speed. Such capabilities are useful for monitoring long-term changes in acquired signals. For example, there is inherent variability in the ACE signal features associated with the ablative state of the targeted tissues that make the tissue state  
20 difficult to track pulse-to-pulse, but characteristic changes in the ACE signals exist over longer treatment time scales (e.g., >20 applied pulses) that allow the ablative state of the tissue to be assessed. One could transfer partial signals in real time to allow localization and mapping of the cavitation events on a per-pulse basis, while storing larger-record length signals on the FPGA to be transferred intermittently to assess the state of the ablation in the therapy target.

**[0121]** In some situations, it is possible to generate focal pressures far in excess of twice what is nominally required to generate cavitation during therapy and in such cases it may be possible to generate cavitation using fewer than half of the histotripsy transducer array elements. The software controlling the histotripsy array allows for the elements of the array to be easily  
25 partitioned into independently controllable sub-apertures, effectively allowing a single physical  
30 histotripsy transducer array to be operated as multiple separate histotripsy arrays. In this way, multiple locations within the focal volume can be targeted for treatment concurrently using the separate sub-apertures of the array, allowing for increases in treatment speed without necessitating an increase in the rate at which pulses are delivered.

## **ABERRATION CORRECTION TECHNIQUES**

**[0122]** Below are described examples of aberration correction methods and techniques that are new and specific for histotripsy therapy.

**[0123]** One embodiment of aberration correction enabled by transmit-receive histotripsy arrays utilizes the arrival time of robust shockwaves emitted by the initial rapid expansion of histotripsy-induced cavitation bubbles. This can be referred to as acoustic cavitation emission (ACE) signals. This shockwave construct emanates spherically from the focal cavitation region back toward the histotripsy therapy array. Any aberrations in the propagation path can be determined by calculating the travel time from the focal cavitation site to each histotripsy array element. After processing the arrival time of the ACE signal received by each element, a correction time delay for each element can be applied to subsequent transmissions for each respective transducer element, such that the ultrasound pulse wave generated by each histotripsy array element will arrive at the focal cavitation position at the same time. This is done by applying the variation in time-of-flight for ACE signals to the transmission pulse signal to each histotripsy array element, such that the transmission signals would arrive at the cavitation site at the same time, correcting the aberration and improving focusing.

**[0124]** For ACE-based aberration correction, a specialized method and algorithm illustrated by the flowchart in FIG. 4 can be implemented that includes the following operations: At step 402, the method can include transmitting histotripsy therapy pulses into a target tissue with an ultrasound transducer array to generate cavitation in the target tissue. As described above, a plurality of transducer elements of the array can each transmit separate histotripsy pulses into the tissue. Next, at operation 404, the method can include receiving acoustic cavitation emissions (ACE signals) resulting from the histotripsy-induced cavitation. The receiving of ACE signals can utilize, for example, any of the systems or drive electronics described above. Next, at an operation 406, the method can use the information encoded in these ACE signals (e.g., start time of the emission generated from cavitation bubble expansion, peak time from cavitation bubble collapse) to calculate the travel time from each element of the histotripsy array to the cavitation in the target tissue. Finally, at operation 408, the method can include adjusting the time delay of the driving electric signal to each array element to correct for the difference in the travel time, such that the ultrasound pulse delivered by each element are configured to arrive at the focus/target tissue at the same time in subsequent transmissions. This method can be used for aberration correction with bones or heterogeneous tissue in the pathway.

**[0125]** Although the method described above discusses receiving ACE transmissions from the rapid expansion of cavitation, the same technique can be used to receive the acoustic shockwave/signals from the cavitation bubble collapse. The signals from the cavitation bubble

collapse received by each array element can be used similarly as the cavitation expansion signals to calculate the time-of-flight for aberration correction as described above.

**[0126]** Shockwave pressure tends to increase linearly with increasing histotripsy focal pressure. One embodiment of the time of flight analysis of these shockwaves involves using the Hilbert transform to calculate an envelope of these shockwaves. A cross-correlation algorithm can then be used to determine the temporal shift required to realign these envelope signals. These temporal shifts are then inverted to correct for variations in time-of-flight across histotripsy elements and are then applied to subsequent pulses as described above. Other methods for analyzing these signals include detecting the peak shockwave pressure or using a window-averaging filter and edge detection algorithm to determine the arrival time of shockwaves. Without aberration correction, the focal pressure at a sub-cavitation threshold amplitude is found to drop to 49.7%, and the transducer power required to induce cavitation triples. Using the ACE aberration correction methods described above, over 20% of the lost pressure can be recovered, and the transducer power required to induce cavitation can be reduced by approximately 31.5%.

**[0127]** Acoustic cavitation emission (ACE) signals may not always be detectable (e.g., due to attenuation effects from propagating through tissues/bone) and/or differentiable from background signals components (e.g., the ACE signals may arrive at the array elements concurrent with histotripsy pulse reflections / reverberations) at sufficient levels to perform aberration correction. In such cases, using the cavitation events as the basis for aberration correction may be achieved using pulse-echo techniques by partitioning the histotripsy array elements into multiple sub-apertures, one of which would be used to generate the cavitation events (sub-aperture A), the other of which would be used to fire interrogation pulses (sub-aperture B). In this scenario, all elements of sub-aperture A would fire histotripsy pulses with sufficient amplitude to generate the cavitation event at the target, say at time = 0. At some time later when the generated cavitation event would have grown in size, say at time = 100us, the elements sub-aperture B would fire pulses directed towards the event. Upon reaching the cavitation event generated by sub-aperture A, the pulses from sub-aperture B would be reflected off of the cavitation event and scattered back towards the array. The array elements of both sub-apertures could then be used to receive the signals reflected off of the cavitation event and the arrival timing of these signals could then be used to calculate the aberration correction delays per the methods described in [69] and [70]. A key benefit of this technique is that the timing of the pulses from sub-aperture B can be set arbitrarily such that the reflected/scattered signals arrive

back at the array elements for detection in a region of the signal where background components are minimal.

**[0128]** In another embodiment, aberration correction can be based on scatter signals from soft tissue.

5 **[0129]** A focal dithering method can also be used for aberration correction based on receive signals. The challenge of using scatter or reflection signals from soft tissue is that the amplitude from the scatter signal from a target tissue is often small and/or buried by the background signals of scatter signals from other tissues. The scattered signals with the array focus at the geometric focus are received from all elements of the array ( $Sc_{1_n}$ ,  $n$  is the element number). Then the array  
10 focus can be dithered to a small distance away (e.g.,  $\frac{1}{2}$  or  $\frac{3}{2}$  wavelength) from the geometric focus, and the scattered signals are also received from all elements of the array ( $Sc_{2_n}$ ,  $n$  is the element number). Both these signals contain the background scatter signals from all heterogeneous tissue in the pathway should, while the difference ( $Sc_{2_n} - Sc_{1_n}$ ) is only due to the scatter signal from the dithered focus with the opposite phase. Combinations of phase or time  
15 delays to all elements will be tested to determine a combination of phase or time delays that can maximize the difference ( $Sc_{2_n} - Sc_{1_n}$ ). This resulted combination can then be used for aberration correction. As the speed of sounds difference between tissue is small, the variations in time-of-flight due to the heterogenous soft tissue path across elements are expected to be small. Thus, a pre-set of combinations of delays can be calculated beforehand to use for testing. This method  
20 allows aberration correction without generating cavitation and potentially maintaining a good enough SNR for processing.

**[0130]** For ultrasound therapy, water is often used as a coupling medium to ensure ultrasound transmission from the transducer array to the skin of the patient. The speed of sound difference between water and soft tissue can result in a substantial location shift of the focus  
25 (e.g., a few millimeters). Reflection signals from the water-skin interface can be received by each array element to determine the time-of-flight from each element surface to the water-skin interface, and use that time-of-flight determination to correct for the focal shift caused by the coupling medium.

**[0131]** Reflection signals from bone can have high amplitudes. The methods and algorithms  
30 described herein can also include detection of transducer elements blocked by ribs (via high amplitude reflected signals) and turning off these transducer elements, or reducing the amplitude of the transmission signals to these transducer elements (amplitude aberration correction) to reduce the potential of rib or bone heating during histotripsy treatment.

[0132] The reflection signals from various tissue surfaces and layers may be received by each array element to model the tissue layers. Based on the speed of sound of each tissue layer using a literature value, the time-of-flight from each element to the array focus may be calculated for aberration correction. This method would only provide a coarse aberration correction.

## 5 CAVITATION LOCALIZATION AND MAPPING

[0133] The ACE signals received by the transmit-receive histotripsy transducer array, described above, can be used to localize and map the cavitation in the target tissue. With the known locations of each histotripsy transducer array element, conventional beamforming methods used in ultrasound imaging and passive cavitation mapping can be used. However, to  
10 image cavitation behind bone or other aberrators, such as the ribs, through the skull, or through deep-overlying tissue, because the speed of sound in the path for each element may vary, modifications to existing beamforming or passive cavitation mapping algorithms are required and discussed herein to account for the travel time variation for different elements to arrive at the focus. The travel time difference can be accounted for using iterative methods to maximize the  
15 signal amplitude within the focal cavitation region after beamforming.

[0134] For example, a brute force method can be used to test a range of ultrasound travel time delays iteratively for all histotripsy array elements. The combination of time delays that results in the highest amplitude of the summed-together ACE signals can then be used for cavitation localization and mapping. This can be achieved sufficiently fast for real-time  
20 imaging. The example below shows a frame rate of 70Hz for cavitation localization through an excised human skull with accuracy within 1.5 mm based on the transmit-receive histotripsy system and the brute force method. It should be noted that the same method can also be used to obtain mapping of the skull surface or ribs that are in the pathway, as the strong reflection signals from the bone can be received by the histotripsy array and separated for processing.

[0135] Example: transcranial cavitation localization and mapping. In this example, a brute force iterative method can be used to localize cavitation through the human skull. The same method can be applied to generate cavitation mapping through the ribs to monitor cavitation behind the ribs. Cavitation localization and mapping are accomplished with the following two steps: 1) signal processing to separate the ACE signals from the skull reflection signals; and 2)  
25 generating a cavitation map by projecting the ACE signals acquired by each element of the array back into the field and summing their signal amplitudes.

[0136] Signal processing to separate the ACE signals from skull reflection signals can include three basic steps. First, low amplitude, sub-cavitation threshold histotripsy pulses can be delivered to the target tissue, and the reflections of the pulses off the intervening tissue can be

recorded using the transducer array elements. These signals can then be scaled up and subtracted from the ACE-containing signals generated after delivering high-amplitude histotripsy pulses in order to isolate the ACE signals from the background. Next, the signals can then be smoothed using a moving window average to reduce spurious effects of noise in the acquired signals on the localization results. The magnitudes of the signals can then be taken as a precondition for a localization algorithm.

**[0137]** Localization and mapping of cavitation events can be accomplished by brute force, iterative methods by projecting the acquired ACE signals back into the field to generate volumetric maps of the projected signal amplitude with the focal region of the transducer. The volumetric maps used in the computations can be generated on grids of voxels centered at the expected locations of the cavitation events in the field. Based on the known locations of the histotripsy transducer elements, and their distances from each voxel in the volumetric grid, the there-and-back times-of-flight of acoustic pulses propagating between the voxels and transducers can be calculated under the assumption that the speed of sound is constant everywhere between them, and having a known speed of sound constant. The signal amplitudes measured from each transducer at the corresponding times at each respective voxel can then be summed together to determine the sum signal amplitude at each voxel. To account for the fact that the sound speed between the transducers and voxels is not constant due to the presence of tissue between them, the process of selecting the time points within the acquired ACE signals from which the measured signal amplitudes were taken can be repeated by iterating in time about the calculated there-and-back times-of-flight at each voxel element and recalculating the signal amplitude field at each time step. The sum signal amplitude at each voxel at the end of the iterative calculations can be taken to be the maximum value calculated at each voxel within the whole iteration window. This process accounts for the combined effects of the tissue sound speed and thickness on ultrasound propagation by considering only the end result, which in this simplified case is to produce a uniform modulation of the signal arrival times at the transducer elements. This greatly reduces computational complexity and allows the effects of tissues to be accounted for during the localization process through iterative time shifting operations. The locations of the cavitation events can then be calculated by finding the center-of-mass of all points within the voxel grid whose amplitudes were >90% of the maximum detected value.

**[0138]** Using this method, 3D cavitation localization can be achieved through bone, such as through ribs or through a human skull. The ACE feedback localization results are accurate to within  $\leq 1.5$  mm of the actual positions of the generated cavitation events' centers-of-mass (as measured through optical imaging). Taking into account the physical sizes of the bubbles,

localization results have been found to fall within <1 mm of the volumes encompassed by the bubbles in >90% of cases. Localization of cavitation in real-time at rates of up to 70 Hz has been achieved during experiments using the described methods, but benchmark tests indicate that the localization algorithm scales efficiently and thus higher rates are likely possible with more powerful hardware.

**[0139]** Referring to FIG. 5A, signals received from each element of the transmit-receive histotripsy array are shown, including the reflection signal from the skull at a sub-threshold cavitation pressure, the skull reflection signal and the ACE signal at a supra-threshold cavitation pressure, and post-processing ACE signals acquired by subtracting the skull reflection signal.

FIG. 5B illustrates a skull surface map and the focal cavitation localization/map produced by processing the ACE signal using the brute-force iterative method.

**[0140]** In another embodiment, the method described for mapping transcranial cavitation is extended for use in applications where targets lie below highly non-uniform aberrators (i.e., the ribs) or where path length variations through tissues en route to the target are significant (e.g., when the transducer must be obliquely aligned with respect to the tissue surface in order to focus at the target). The same signal processing and localization methods as described above can be applied with two important additions.

**[0141]** Signal Processing: An additional step in the signal processing may be required to account for the presence of non-uniform aberrators and oblique surfaces. First, each element of the array is fired individually, and the reflections of the pulses off of the tissue(s) are recorded by all array elements. Given the known positions of the transducer elements and sound speed of the coupling medium, traditional delay sum beamforming can be used to generate a 3D map of the tissue surface and underlying features (i.e., the ribs) from the acquired signals.

**[0142]** 2) Cavitation Localization and mapping: Given the known surface geometry of the tissue, and/or locations of underlying features such as the ribs, non-uniform delays can be applied to the ACE signals acquired during the time-iteration process used to localize the cavitation events. In the case of ribs, based on their known positions, the delays assigned to the ACE signals known to propagate through ribs can be assigned a fixed offset with respect to those that don't, in order to maximize the projected signal amplitude in the field to localize the cavitation event. Or, given the known surface geometry of the tissue with respect to an obliquely aligned transducer, the time-delays assigned to each element can be set in a graduated way to account for the different path lengths of tissue through which the ACE signals would need to travel in order to reach each array element.

[0143] In another embodiment, the methods described are extended for use in applications where targets lie within an approximately uniform aberrator (i.e., the liver) whose sound speed may not be well known, particularly where path length variations through tissues en route to the target are significant (e.g., when the transducer must be obliquely aligned with respect to the tissue surface in order to focus at the target). The same signal processing and localization methods as described, as well as method for mapping the tissue surface geometry described above can be applied with the following addition.

[0144] Given the known surface geometry of the tissue, sound speed of the coupling medium, and timings of the generated ACE signals, the location of the cavitation events as well as the sound speed of the nucleation medium itself can be determined via minimization of a coupled system of equations through the application of Snell's law describing refraction. Given the known positions of the array elements with respect to the tissue surface, the time of flight from each element to every point on the tissue surface, and the respective trajectories of the pulses with respect to it, can be calculated. Upon exiting the tissue, the trajectory of the ACE signal from the cavitation event will be altered due to the difference in sound speeds between the tissue and the coupling medium per Snell's law. The sound speed of the coupling medium, and distance from the array elements to every point on the tissue surface are known, but not which point on the tissue surface the received portion of the ACE signal acquired by each array element originated from; the sound speed of the tissue and the location of the cavitation event being mapped are also unknown. The timings of the ACE signals at the individual array elements,  $t_{ACE,n}$ , will only depend on the distance propagated through the coupling medium and the tissue, and their respective sound speeds as  $t_{ACE,n} = [D_{cm,n}/C_{cm,n} + D_{t,n}/C_{t,n}]$ , where the 'D' and 'C' correspond to the 'distance traveled' and 'sound speed of the medium', respectively, and the subscripts 'cm', 't', and 'n' correspond to 'coupling medium', 'tissue', and 'element number' respectively. The values of three of these variables ( $D_{cm,n}$ ,  $D_{t,n}$ ,  $C_{t,n}$ ) are unknown, however, the value of  $D_{cm,n}$  becomes immaterial through the enforcement of Snell's law at the tissue-coupling medium boundary because it can be re-expressed purely in terms of the values of  $D_{t,n}$  and  $C_{t,n}$  once they are known. One can then solve for the sound speed of the medium and the location of the generated cavitation by minimizing the value returned by  $\sum t_{ACE,n,exp} - t_{ACE,n}$ , where  $t_{ACE,n,exp}$  is the experimentally measured timing of the ACE signal, through adjusting the values of  $C_{t,n}$  and the location of the cavitation bubble in the tissue (which is expressed through the value of  $D_{t,n}$ ).

### REAL-TIME TREATMENT MONITORING

[0145] As discussed above, histotripsy generates cavitation to mechanically fractionate target tissue. With increasing dosage or therapy, treated tissue becomes increasingly soft and

eventually liquefied into an acellular debris. As a result, over the course of treatment, the cavitation bubbles generated grow larger, take a longer time to collapse, and eventually the cavitation activity mimics strong cavitation activity in fluid. The cavitation expansion and collapse signals can be detected via the acoustic cavitation emission (ACE) signals received by the transmit-receive histotripsy array, which can then be processed to quantitatively monitor the treatment progression and determine the treatment completion. For example, the time to maximum cavitation bubble growth and bubble collapse time increase over the treatment and eventually saturate when the target tissue is liquefied and the treatment is complete. This increasing trend can be detected by processing ACE via specific algorithms to indicate when the treatment is progressing, and the saturation trend can be detected by specific algorithms to determine the treatment is completed, all in real-time. Examples of such algorithms might include using peak detection in the acquired waveforms individually to identify the ACE signals associated with the bubble's growth and collapse, and measuring the timing between them. In cases where signals are embedded within strong background environments, individual waveforms can be processed via autocorrelation to identify the timings between self-similar regions within the waveforms (i.e., the growth and collapse ACE signals). As the background environments of the individual signals would not be equivalent to each other, the ACE signals could then be identified by comparing all of the individual autocorrelation results from each array element with each other, for example by median filtering them, which would show consistent peaks at the time corresponding to the bubble's lifespan. Backprojecting the acquired signals into the field to image for the volume as a function of time would similarly show peaks in the projected signal amplitudes within the image-formed volumes at times corresponding the growth and collapse ACE signals.

**[0146]** However, the acoustics of these ACE signals are very complicated and can be analyzed in many different ways to obtain desired metrics for treatment progression monitoring. Therefore, specialized algorithms are needed, which include the following functions. Referring to the flowchart of FIG. 6, a method of histotripsy treatment progression monitoring can include, at step 602, detecting a selected ACE feature (e.g., the timings and amplitudes of the cavitation bubble expansion signals, collapse signals, and/or rebound signals) to separate from tissue signals, at step 604, calculating a cavitation parameter (e.g., collapse time i.e., the time between the expansion signal and collapse signal, peak amplitude of the expansion signal, peak amplitude of the collapse signal, amplitude ratios of the growth and collapse ACE signals, or the decay rates of the rebound-associated ACE signal amplitudes) that correlates to the tissue damage generated by histotripsy, at step 606, determining a change (e.g., increasing slope of the selected

cavitation parameter) that correlates to normal treatment progression, and at step 608, determining a change (e.g., saturation of the change of the selected cavitation parameter) that correlates to treatment completion.

**[0147]** An example of the cavitation parameter collapse time is provided. This example shows that the increase and saturation of the cavitation collapse time is correlated with the treatment progression and completion. The change in the collapse time ( $t_{col}$ ) of the cavitation bubble cloud over the histotripsy treatment is an indicator for progression of the tissue fractionation process during the histotripsy treatment.

**[0148]** In an experiment, 500-kHz, 112-element histotripsy array was used to generate single-location lesions within tissue-mimicking agar phantoms of varying stiffness levels as well as ex vivo bovine liver samples. Cavitation collapse signals were received, and cavitation was imaged using a high-speed camera in transparent tissue-mimicking phantoms. The high-speed-camera-acquired measurements of  $t_{col}$  optically validate the acoustic hydrophone measurements. Increases in  $t_{col}$  are observed both with decreasing phantom stiffness and throughout histotripsy treatment with increasing number of pulses applied. The increasing trend of  $t_{col}$  throughout the histotripsy treatment correlated well with the progression of lesion formation generated in tissue-mimicking phantoms ( $R^2 = 0.87$ ) (FIG. 7). Referring to FIG. 7,  $t_{col}$  (left y-axis) and mean lesion intensity (MLI) (right y-axis) vs. pulse number throughout 100 pulses are shown. The MLI, defined as the average pixel intensity over the ROI, was calculated for the entire treatment on a normalized scale from 0 to 1 to indicate the treatment progress (0 – no treatment; 1 – treatment completion). The majority of changes in  $t_{col}$  and MLI occur early in treatment and at the same time. The change in  $t_{col}$  is greater than the change in MLI in the first several pulses, but both metrics even out quickly and reach a plateau threshold around 40 pulses.

**[0149]** Finally, the increasing trend of  $t_{col}$  over the histotripsy treatment was validated in ex vivo bovine liver. The  $t_{col}$  experienced an overall average increase of approximately 50  $\mu$ s throughout treatment, and it reached this steady-state value around 40 to 50 histotripsy pulses (FIGS. 8A-8B). In FIGS. 8A-8B, collapse time  $t_{col}$  for first 100 pulses (right, linear scale) and 1000 pulses (left, log scale) in ex vivo bovine liver ( $n=4$ ) are shown. The majority of the change in  $t_{col}$  is observed within the first 100 pulses of treatment with little to no change between pulse 100 and pulse 1000.

**[0150]** The acoustic cavitation emission (ACE) signal generated by the cavitation cloud during histotripsy therapy was also investigated as a potential feedback mechanism for tissue integrity during treatment. A 500-kHz, 112-element phased histotripsy array was used to generate approximately 6x6x7 mm lesions within ex vivo bovine liver tissue by scanning over

219 locations with 30-1000 pulses-per-location. A custom nonlinear voltage compressor was designed and constructed to allow 8 elements of the array to transmit histotripsy pulses and receive ACE signals from the central treatment location within the lesion. The ACE signal was quantitatively analyzed by measuring the change in the peak pressure arrival time throughout treatment. The ACE peak pressure arrival time decreased as the treatment progressed and eventually saturated (FIG. 9). Referring to FIG. 9, quantified ACE using the peak pressure arrival time is shown. The trend exhibited by the peak pressure arrival throughout treatment suggests that the majority of physical changes that influence this metric occur in the first 200 pulses. A nonlinear least squares best-fit line is shown in black. The best-fit line reached an exponential decay time constant at 80 pulses.

**[0151]** The histology of the treated tissue was analyzed, and correspondingly the cell count, reticulin-stained type III collagen area, and trichrome-stained type I collagen area all decreased over the course of histotripsy treatment (FIG. 10). Using the Pearson correlation coefficient (PCC), the ACE signal was compared to histological analytics of lesions generated by different numbers of pulses using a significance level of 0.05. Histological analytics included viable cell count, reticulin-stained type III collagen area, and trichrome-stained type I collagen area. It was found that the decrease of the peak pressure arrival time had a statistically significant correlation with the reduction in reticulin-stained type III collagen area with a PCC of 0.72 ( $p = 0.043$ ). This indicates the feasibility of using the ACE peak pressure arrival time as an indicator for histotripsy treatment monitoring. The transmit-receive hardware and software can be significantly improved to improve the sensitivity of this detection. Referring to FIG. 10, a histological analysis of 42 histotripsy treated samples at varying dosages is shown. FIG. 10A shows a viable cell count remaining in imaged medium. The cell count experienced the greatest amount of destruction early in treatment. FIG. 10B shows a percent area with intact reticulin-stained collagen and FIG. 10C shows a percent area with intact trichrome-stained collagen. Both collagen metrics experienced slower amounts of destruction than remaining cell count. Nonlinear least square best-fit lines are shown in red. All best fit lines exhibited statistical significance when compared to a normal distribution as indicated by the p-values on each plot.

**[0152]** The advantages of the transmit-receive histotripsy phased array as described herein can be summarized as following.

**[0153]** 1) Aberration correction - Transmit-receive histotripsy can correct aberration due to the speed of sound variation in the ultrasound pathway and improve focusing. As correction needs to be applied to each array element, the correction methods based on the signal received by each element provides the most accurate aberration correction. The advanced transmit-receive

histotripsy hardware and software along with the specialized aberration correction algorithms can enable aberration correction on-the-fly immediately before or even during the treatment.

5 [0154] 2) Cavitation localization and mapping - As cavitation is the causative agent for histotripsy to generate damage, the real-time, 3D cavitation map can facilitate targeting and treatment monitoring, even with ribs or skull in the pathway. The 3D cavitation map would also allow us to detect both intended cavitation at the target and any potential unwanted off-target cavitation. Therefore, the real-time 3D feedback provided by the transmit-receive histotripsy transducer array can overcome the two main limitations of the ultrasound imaging feedback as described earlier.

10 [0155] 3) Treatment monitoring - Cavitation dynamics are correlated to the level of tissue damage generated by histotripsy. The received ACE signals can be processed to monitor the treatment progress and determine the completion of the treatment in real-time. The 3D cavitation mapping can also be co-registered or overlaid onto a pre-treatment MRI or CT scan.

15 [0156] 4) Compact system - The transmit-receive histotripsy array system can be compact and of similar size of a transmit-only histotripsy system, but with many added features as described above. The transmit-receive histotripsy array can be used independent of and/or supplemental to the ultrasound imaging that is currently used for histotripsy feedback.

20 [0157] 5) Automatic registration - The map of cavitation generated by the transducer receive is automatically registered to the therapy side coordinate system. The treatment accuracy then only relies on a single registration between therapy transducer and treatment planning imaging.

## METHODS OF USE

25 [0158] The transmit-receive ultrasound systems described herein can enable ultrasound and/or histotripsy therapy that provides general amplitude aberration correction to make therapy more efficient, and can further provide corrections for focal shift. These methods are described below:

[0159] General amplitude aberration correction

30 [0160] Methods of providing general amplitude aberration correction during ultrasound therapy are provided. These methods can include transmitting ultrasound pulses into a single test pulse location (e.g., the center of the planned treatment volume aligned with the target tissue), and receiving time delays from the single location. Next, the received time delays can be used as a representative aberration correction map for the entire planned treatment volume (e.g., all treatment pattern locations within the planned treatment volume). Aberration correction can then be applied to subsequent ultrasound treatment pulses to increase efficiency of the therapy.

**[0161]** In some examples, multiple discrete test pulse locations can be used (e.g., seven-point test locations). The method can include receiving time delays at each test location/position and modeling the received delays to interpolate the aberration correction map for the entire planned treatment volume.

5 **[0162]** Alternatively, the method can include real-time testing. For example, the method can include using received signals for aberration correction at each test pulse and treatment location and updating the aberration correction in real-time during therapy.

**[0163]** In some examples, test pulse sequences can be different than therapy pulses (automated treatment) to afford smaller clouds or more thermally favorable sequences to assess  
10 aberration/threshold, before transitioning to therapy pulses.

**[0164]** *Correcting for focal shift*

**[0165]** During ultrasound/histotripsy therapy, it is common to see a focal shift, typically along the “Z” axis and mostly due to the difference of sound speed in water (coupling medium) and tissue. This can typically be corrected for in the ultrasound system by visualizing the bubble  
15 cloud with an imaging system (e.g., ultrasound imaging). As described herein, the receive capability of the system can be used to map the reflection signals from the water-skin interface to determine the time-of-flight from each element surface to the water-skin interface, and use that time-of-flight determination to correct for the focal shift caused by the coupling medium.

**[0166]** To build and expand upon this method, other inputs can be used to make the  
20 prediction of focal shift more accurate. For example, focal shift correction can be based on a single test pulse at (e.g., at the center of the planned treatment volume), or based on multiple test-pulses interpolated over the volume.

**[0167]** The receive data received by the system can be registered with imaging data from an imaging system to provide more visual feedback regarding cavitation. Additionally, the receive  
25 and imaging data can be registered with the robotic positioning arm of the therapy system so the image/receive data is in context to the six degrees of freedom of the positioning arm.

**[0168]** The methods described above can be used to correct for focal shift/aberration when the imaging system is obscured (such as when the focal zone is behind bone or another aberrator).

30 **[0169]** When a feature or element is herein referred to as being “on” another feature or element, it can be directly on the other feature or element or intervening features and/or elements may also be present. In contrast, when a feature or element is referred to as being “directly on” another feature or element, there are no intervening features or elements present. It will also be understood that, when a feature or element is referred to as being “connected”, “attached” or

“coupled” to another feature or element, it can be directly connected, attached or coupled to the other feature or element or intervening features or elements may be present. In contrast, when a feature or element is referred to as being “directly connected”, “directly attached” or “directly coupled” to another feature or element, there are no intervening features or elements present.

5 Although described or shown with respect to one embodiment, the features and elements so described or shown can apply to other embodiments. It will also be appreciated by those of skill in the art that references to a structure or feature that is disposed “adjacent” another feature may have portions that overlap or underlie the adjacent feature.

[0170] Terminology used herein is for the purpose of describing particular embodiments  
10 only and is not intended to be limiting of the invention. For example, as used herein, the singular forms “a”, “an” and “the” are intended to include the plural forms as well, unless the context clearly indicates otherwise. It will be further understood that the terms “comprises” and/or “comprising,” when used in this specification, specify the presence of stated features, steps, operations, elements, and/or components, but do not preclude the presence or addition of one or  
15 more other features, steps, operations, elements, components, and/or groups thereof. As used herein, the term “and/or” includes any and all combinations of one or more of the associated listed items and may be abbreviated as “/”.

[0171] Spatially relative terms, such as “under”, “below”, “lower”, “over”, “upper” and the like, may be used herein for ease of description to describe one element or feature’s relationship  
20 to another element(s) or feature(s) as illustrated in the figures. It will be understood that the spatially relative terms are intended to encompass different orientations of the device in use or operation in addition to the orientation depicted in the figures. For example, if a device in the figures is inverted, elements described as “under” or “beneath” other elements or features would then be oriented “over” the other elements or features. Thus, the exemplary term “under” can  
25 encompass both an orientation of over and under. The device may be otherwise oriented (rotated 90 degrees or at other orientations) and the spatially relative descriptors used herein interpreted accordingly. Similarly, the terms “upwardly”, “downwardly”, “vertical”, “horizontal” and the like are used herein for the purpose of explanation only unless specifically indicated otherwise.

[0172] Although the terms “first” and “second” may be used herein to describe various  
30 features/elements (including steps), these features/elements should not be limited by these terms, unless the context indicates otherwise. These terms may be used to distinguish one feature/element from another feature/element. Thus, a first feature/element discussed below could be termed a second feature/element, and similarly, a second feature/element discussed

below could be termed a first feature/element without departing from the teachings of the present invention.

**[0173]** Throughout this specification and the claims which follow, unless the context requires otherwise, the word “comprise”, and variations such as “comprises” and “comprising” means various components can be co-jointly employed in the methods and articles (e.g., compositions and apparatuses including device and methods). For example, the term “comprising” will be understood to imply the inclusion of any stated elements or steps but not the exclusion of any other elements or steps.

**[0174]** As used herein in the specification and claims, including as used in the examples and unless otherwise expressly specified, all numbers may be read as if prefaced by the word “about” or “approximately,” even if the term does not expressly appear. The phrase “about” or “approximately” may be used when describing magnitude and/or position to indicate that the value and/or position described is within a reasonable expected range of values and/or positions. For example, a numeric value may have a value that is +/- 0.1% of the stated value (or range of values), +/- 1% of the stated value (or range of values), +/- 2% of the stated value (or range of values), +/- 5% of the stated value (or range of values), +/- 10% of the stated value (or range of values), etc. Any numerical values given herein should also be understood to include about or approximately that value, unless the context indicates otherwise. For example, if the value “10” is disclosed, then “about 10” is also disclosed. Any numerical range recited herein is intended to include all sub-ranges subsumed therein. It is also understood that when a value is disclosed that “less than or equal to” the value, “greater than or equal to the value” and possible ranges between values are also disclosed, as appropriately understood by the skilled artisan. For example, if the value “X” is disclosed the “less than or equal to X” as well as “greater than or equal to X” (e.g., where X is a numerical value) is also disclosed. It is also understood that the throughout the application, data is provided in a number of different formats, and that this data, represents endpoints and starting points, and ranges for any combination of the data points. For example, if a particular data point “10” and a particular data point “15” are disclosed, it is understood that greater than, greater than or equal to, less than, less than or equal to, and equal to 10 and 15 are considered disclosed as well as between 10 and 15. It is also understood that each unit between two particular units are also disclosed. For example, if 10 and 15 are disclosed, then 11, 12, 13, and 14 are also disclosed.

**[0175]** Although various illustrative embodiments are described above, any of a number of changes may be made to various embodiments without departing from the scope of the invention as described by the claims. For example, the order in which various described method steps are

performed may often be changed in alternative embodiments, and in other alternative embodiments one or more method steps may be skipped altogether. Optional features of various device and system embodiments may be included in some embodiments and not in others.

Therefore, the foregoing description is provided primarily for exemplary purposes and should  
5 not be interpreted to limit the scope of the invention as it is set forth in the claims.

**[0176]** The examples and illustrations included herein show, by way of illustration and not of limitation, specific embodiments in which the subject matter may be practiced. As mentioned, other embodiments may be utilized and derived there from, such that structural and logical substitutions and changes may be made without departing from the scope of this disclosure.  
10 Such embodiments of the inventive subject matter may be referred to herein individually or collectively by the term “invention” merely for convenience and without intending to voluntarily limit the scope of this application to any single invention or inventive concept, if more than one is, in fact, disclosed. Thus, although specific embodiments have been illustrated and described herein, any arrangement calculated to achieve the same purpose may be substituted for the  
15 specific embodiments shown. This disclosure is intended to cover any and all adaptations or variations of various embodiments. Combinations of the above embodiments, and other embodiments not specifically described herein, will be apparent to those of skill in the art upon reviewing the above description.

## CLAIMS

**What is claimed is:**

1. A transmit-receive driving electronics for a histotripsy system, comprising:  
at least one transducer element configured to transmit ultrasound pulses in a transmit  
5 mode and receive ultrasound reflections and/or acoustic cavitation emissions in a receive mode;  
a current sense resistor configured to measure a current in the transmit-receive driving  
electronics during the receive mode;  
a bypass circuit electrically coupled to the at least one transducer element and the current  
sense resistor, wherein the bypass circuit is configured to be switched on during the transmit  
10 mode to bypass the current sense resistor and switched off during the receive mode to allow the  
sense resistor to measure the current; and  
a gain adjustment circuit electrically coupled to the current sense resistor and to a low  
sensitivity resistor, the gain adjustment circuit being configured to operate in a high sensitivity  
setting in which the current sense resistor is switched on and the low sensitivity resistor is  
15 switched off, and wherein the gain adjustment circuit is further configured to operate in a low  
sensitivity setting in which the current sense resistor and the low sensitivity resistor are switched  
on.
2. The transmit-receive driving electronics of claim 1, further comprising:  
20 a drive transformer electrically coupled to the at least one transducer element.
3. The transmit-receive driving electronics of claim 1, wherein the bypass circuit further  
comprises a pair of bypass transistors.
- 25 4. The transmit-receive driving electronics of claim 1, wherein the bypass circuit further  
comprises a pair of bypass diodes.
5. The transmit-receive driving electronics of claim 1, wherein the gain adjustment circuit  
further comprises a pair of transistors.
- 30 6. The transmit-receive driving electronics of claim 1, wherein the current sense resistor has  
a higher resistance than the low sensitivity resistor.

7. The transmit-receive driving electronics of claim 1, wherein the current sense resistor has a resistance of approximately 200 ohms and the low sensitivity resistor has a resistance of approximately 5 ohms.
- 5 8. A transmit-receive driving electronics for a histotripsy system, comprising:  
an ultrasound transducer array;  
high-voltage transmission electronics coupled to the ultrasound transducer array and configured to provide up to thousands of volts to the ultrasound transducer array to produce one or more histotripsy pulses;
- 10 first receive electronics coupled to the ultrasound transducer array and configured to receive incoming voltage signals from the transmitted one or more histotripsy pulses, the first receive electronics being configured to attenuate the incoming voltage signals by 90-99%;  
second receive electronics configured to compress any attenuated incoming voltage signals above 1V;
- 15 third receive electronics configured to voltage shift the attenuated incoming voltage signals; and  
an analog-to-digital converter configured to receive the voltage-shifted attenuated incoming voltage signals from the third receive electronics for ADC conversion.
- 20 9. The transmit-receive driving electronics of claim 8, wherein the first electronics comprise a voltage divider.
10. The transmit-receive driving electronics of claim 9, wherein the voltage divider comprises a capacitive voltage divider.
- 25 11. The transmit-receive driving electronics of claim 10, wherein the capacitive voltage divider comprises a first capacitor and a second capacitor in parallel with a first transducer element of the ultrasound transducer array.
- 30 12. The transmit-receive driving electronics of claim 8, wherein the second receive electronics comprise a diode-resistor voltage divider.

13. The transmit-receive driving electronics of claim 8, wherein the third receive electronics are configured to voltage shift the attenuated incoming voltage signals to an appropriate voltage range for the analog-to-digital converter.
- 5 14. The transmit-receive driving electronics of claim 8, wherein the transmit-driving electronics comprise a separate circuitry board that is configured to be retrofitted to an existing histotripsy system that includes a transmit-only histotripsy driving system.
- 10 15. The transmit-receive driving electronics of claim 14, wherein the transmit-driving electronics is added in parallel to the transmit-only histotripsy driving system and is configured to passively receive signals without affecting the transmit-only electronics.
- 15 16. The transmit-receive driving electronics of claim 8, being further configured to synchronize a time clock of the transmitted one or more histotripsy pulses, received incoming voltage signals, and the ADC conversion to obtain an appropriate time window after each histotripsy pulse transmission.
- 20 17. The transmit-receive driving electronics of claim 8, further comprising one or more Field Programmable Gate Array (FPGA) boards coupled to the analog-to-digital converter and being configured to control transmit and receive operations of the transmit-receive driving electronics with a single clock.
- 25 18. The transmit-receive driving electronics of claim 17, wherein the one or more FPGA includes software or firmware configured to reduce a data load for received signals.
19. The transmit-receive driving electronics of claim 17, wherein the one or more FPGA are configured to artificially downsample incoming data from the analog-to-digital converter.
- 30 20. The transmit-receive driving electronics of claim 17, wherein the one or more FPGA are configured to oversample and average the received signals to increase a signal to noise ratio (SNR).
21. A method of using a transmit-receive histotripsy system for cavitation detection, comprising the steps of:

transmitting high-voltage histotripsy therapy pulses into a target tissue with transmit electronics and a histotripsy therapy transducer array to generate cavitation in the target tissue; receiving low-voltage acoustic cavitation emission signals from the cavitation with receive electronics and the histotripsy therapy transducer array; and  
5 processing the received acoustic cavitation emission signals to monitor treatment progression.

22. The method of claim 21, further comprising generating a 3D map of cavitation produced by the transmitted pulses in real-time.

10

23. A method of using a transmit-receive histotripsy system for aberration correction, comprising the steps of:

transmitting histotripsy therapy pulses into a target tissue with a histotripsy therapy transducer array having a plurality of transducer elements to generate cavitation in the target  
15 tissue;

receiving acoustic cavitation emission signals from the cavitation with the histotripsy therapy transducer array;

calculating a travel time from the cavitation to each transducer element of the ultrasound transducer array based on the received acoustic cavitation emission signals; and

20

adjusting a transmission time delay for at least one of the plurality of transducer elements based on the calculated travel times such that subsequent histotripsy therapy pulses arrive at the target tissue simultaneously.

24. The method of claim 23, wherein calculating the travel time includes using information  
25 encoded in the acoustic cavitation emissions.

25. The method of claim 24, wherein the information comprises a start time of the acoustic cavitation emission generated from cavitation expansion.

30 26. The method of claim 24, wherein the information comprises a start time of the acoustic cavitation emission generated from cavitation collapse.

27. The method of claim 24, wherein the information comprises a peak time from cavitation collapse.

28. A receive-drive circuit configured to be retrofitted onto one or more transducer elements of an existing transmit-only histotripsy system, comprising:
- a voltage divider configured to be electrically coupled to a first transducer element, the
  - 5 voltage divider configured to attenuate voltage signals received by the first transducer element; and
  - a diode-resistor voltage divider electrically coupled to the voltage divider, the diode-resistor voltage divider being configured to provide nonlinear attenuation to compress signals above a predetermined voltage, and being further configured to AC couple the received signals
  - 10 to an analog to digital converter.
29. The receive-drive circuit of claim 28, wherein the voltage divider and the diode-resistor voltage divider are configured to be disposed on a first circuitry board and that is configured to be electrically coupled to high-voltage histotripsy driving electronics disposed on a separate
- 15 second circuitry board.
30. The receive-drive circuit of claim 28, wherein the receive-drive circuit and high-voltage histotripsy driving electronics are disposed on a single circuitry board.
- 20 31. A transmit-receive histotripsy system, comprising:
- a transducer element;
  - transmit electronics coupled to the transducer element and configured to deliver histotripsy pulses to the transducer element; and
  - a non-linear compressor receive electronics coupled to the transducer element, wherein
  - 25 the non-linear compressor receive electronics are configured to compress a first voltage signal with a first attenuation, and are further configured to compress a second voltage signal with a second attenuation, wherein the first voltage signal is higher than the second voltage signal and the first attenuation is higher than the second attenuation.
- 30 32. A transmit-receive driving electronics for a histotripsy system, comprising:
- a transducer element;
  - a secondary transformer coil electrically coupled to the transducer element;

a primary transformer coil positioned adjacent to the secondary transformer coil, the primary transformer coil being configured to generate ultrasound pulses in the transducer element via the secondary transformer coil; and

5 a third transformer coil positioned adjacent to the secondary transformer coil, the third transformer coil being configured to attenuate voltage signals received by the transducer element by a predetermined amount.

33. The transmit-receive drive electronics of claim 32, wherein the third transformer coil is configured to attenuate the received voltage signals by 90-99%.

10

34. The transmit-receive drive electronics of claim 33, wherein the third transformer coil is wound with approximately 7-10x fewer windings than the secondary transformer coil.

35. The transmit-receive drive electronics of claim 32, wherein the third transformer coil is configured to saturate during transmission of ultrasound pulses.

15

36. The transmit-receive drive electronics of claim 35, wherein the third transformer coil is coupled to a signal transformer with a specifically chosen core material and size such that the signal transformer is configured to saturate during transmission of ultrasound pulses.

20

37. A transmit-receive driving electronics of a histotripsy system, comprising:

an ultrasound transducer array;

transmission electronics coupled to the ultrasound transducer array and configured to transmit one or more histotripsy pulses to generate cavitation in a target tissue;

25 receive electronics configured to receive acoustic cavitation emissions from the cavitation; and

a transmit-receive switch configured to enable only the transmission electronics during transmission of the one or more histotripsy pulses, the transmit-receive switch being further configured to enable only the receive electronics at a predetermined time after the transmission of the one or more histotripsy pulses, to block transmission signals without attenuating received signals.

30

38. The transmit-receive driving electronics of claim 37, wherein a different linear gain follows the transmit-receive switch to amplify or attenuate a selected portion of the received signal based on its amplitude to maximize a receive sensitivity of the receive electronics.
- 5 39. A method histotripsy therapy, comprising the steps of:  
transmitting histotripsy therapy pulses into a target tissue with a histotripsy therapy transducer array to generate cavitation in the target tissue;  
receiving acoustic cavitation emission signals from the cavitation with the histotripsy therapy transducer;
- 10 detecting a selected acoustic cavitation emission feature to separate from tissue signals;  
calculating a cavitation parameter that correlates to tissue damage generated by the histotripsy therapy pulses;  
determining a change in the cavitation parameter that correlates to treatment progression;  
and
- 15 determining a change in the cavitation parameter that correlates to treatment completion.
40. The method of claim 39, wherein the selected acoustic cavitation emission feature comprises a timing of cavitation bubble expansion signals.
- 20 41. The method of claim 39, wherein the selected acoustic cavitation emission feature comprises an amplitude of cavitation bubble expansion signals.
42. The method of claim 39, wherein the selected acoustic cavitation emission feature comprises a timing of cavitation bubble collapse signals.
- 25 43. The method of claim 39, wherein the selected acoustic cavitation emission feature comprises an amplitude of cavitation bubble collapse signals.
44. The method of claim 39, wherein the selected acoustic cavitation emission feature
- 30 comprises a timing of cavitation bubble rebound signals.
45. The method of claim 39, wherein the selected acoustic cavitation emission feature comprises an amplitude of cavitation bubble rebound signals.

46. The method of claim 39, wherein the cavitation parameter comprises a collapse time of the cavitation.
47. The method of claim 46, wherein the collapse time comprises a time between expansion and collapse signals of the cavitation.
48. The method of claim 39, wherein the cavitation parameter comprises a peak amplitude of an expansion signal of the cavitation.
49. The method of claim 39, wherein the cavitation parameter comprises a peak amplitude of a collapse signal of the cavitation.
50. The method of claim 39, wherein the cavitation parameter comprises amplitude ratios of a growth ACE signal of the cavitation.
51. The method of claim 39, wherein the cavitation parameter comprises amplitude ratios of a collapse ACE signal of the cavitation.
52. The method of claim 39, wherein the cavitation parameter comprises a decay rate of rebound-associated ACE signal amplitudes.
53. The method of claim 39, wherein determining a change in the cavitation parameter that correlates to treatment progression further comprises identifying an increasing slope in the cavitation parameter.
54. The method of claim 39, wherein determining a change in the cavitation parameter that correlates to treatment completion further comprises identifying saturation of the change in the cavitation parameter.
55. A method for cavitation detection during histotripsy, comprising the steps of:  
transmitting histotripsy therapy pulses into a target tissue with a histotripsy therapy transducer array to generate cavitation in the target tissue;  
receiving acoustic cavitation emission signals from the cavitation with the histotripsy therapy transducer array;

detecting a selected acoustic cavitation emission feature to separate from tissue signals;  
processing and forming a cavitation map based on the selected acoustic cavitation  
emission feature; and  
overlaying the cavitation map onto an image of the target tissue.

5

56. The method of claim 55, wherein the selected acoustic cavitation emission feature  
comprises a timing of cavitation bubble expansion signals.

57. The method of claim 55, wherein the selected acoustic cavitation emission feature  
10 comprises an amplitude of cavitation bubble expansion signals.

58. The method of claim 55, wherein the selected acoustic cavitation emission feature  
comprises a timing of cavitation bubble collapse signals.

15 59. The method of claim 55, wherein the selected acoustic cavitation emission feature  
comprises an amplitude of cavitation bubble collapse signals.

60. The method of claim 55, wherein the selected acoustic cavitation emission feature  
comprises a timing of cavitation bubble rebound signals.

20

61. The method of claim 55, wherein the selected acoustic cavitation emission feature  
comprises an amplitude of cavitation bubble rebound signals.

25 62. A method of performing aberration correction during histotripsy therapy, comprising the  
steps of:

transmitting histotripsy therapy pulses into a target tissue with a histotripsy therapy  
transducer array to generate cavitation in the target tissue;

receiving acoustic cavitation emission signals from the cavitation with the histotripsy  
therapy transducer array;

30 analyzing the acoustic cavitation emission signals to detect the cavitation generated in the  
target tissue;

testing presets of transmission time delays to select a set of transmission time delays that  
can maximize a peak signal amplitude in the detected cavitation; and

applying the selected set of transmission time delays such that subsequent histotripsy therapy pulses arrive at the target tissue simultaneously.

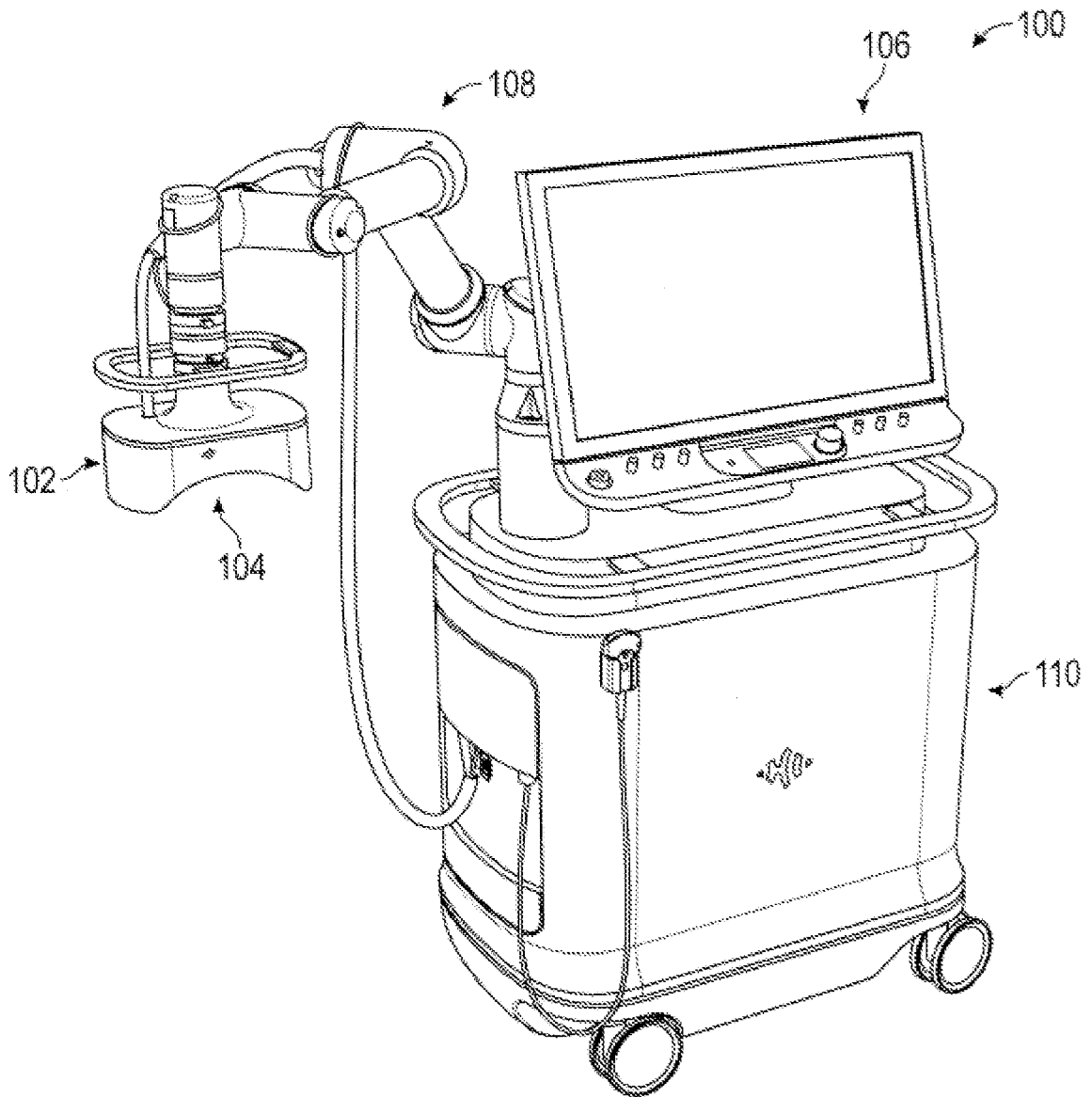


FIG. 1A

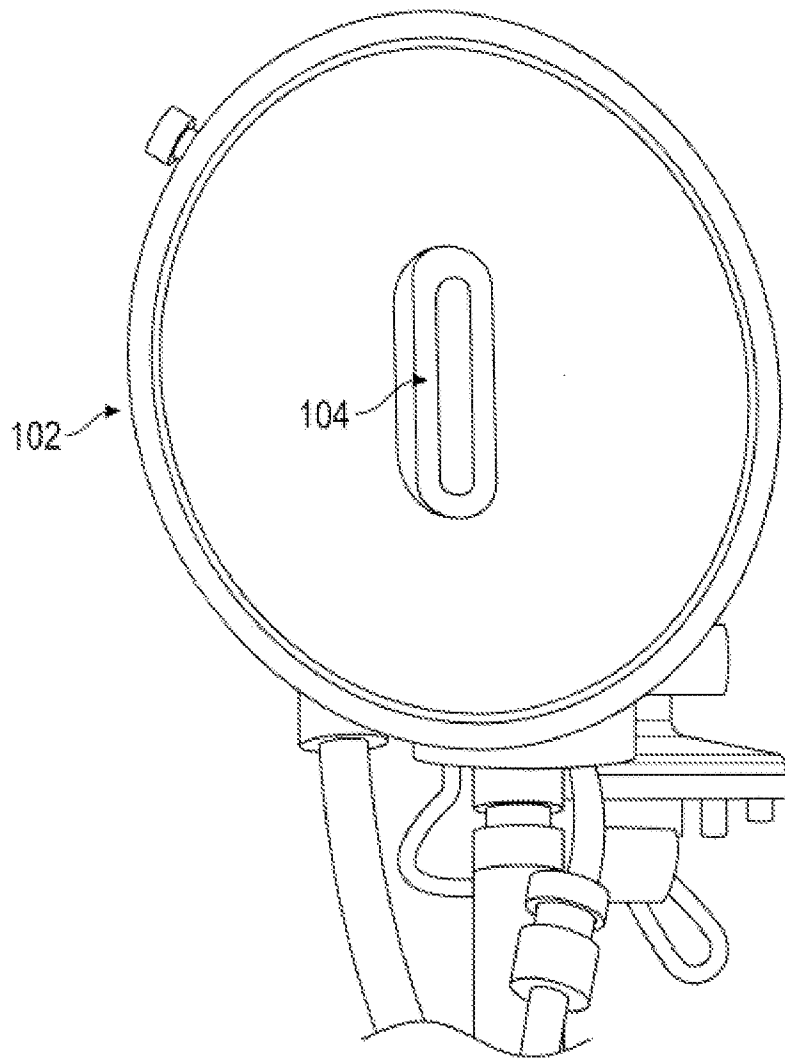


FIG. 1B

FIG. 2A

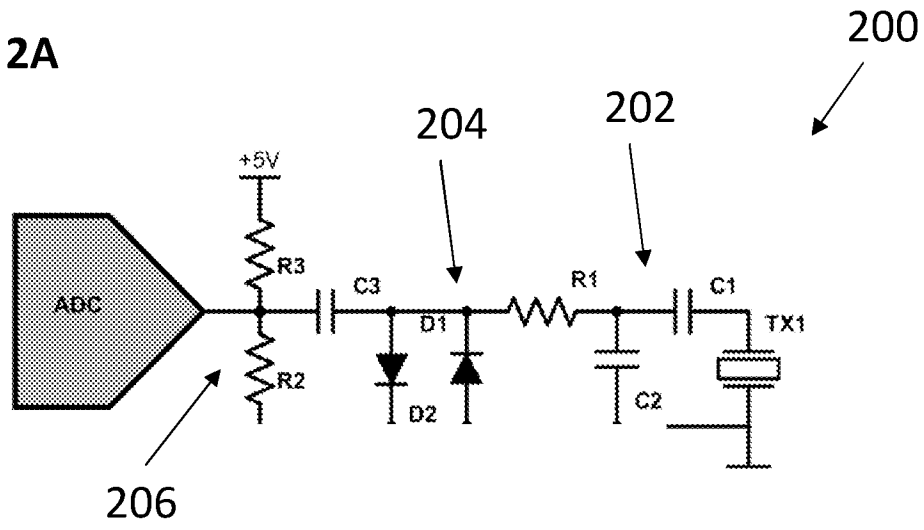


FIG. 2B

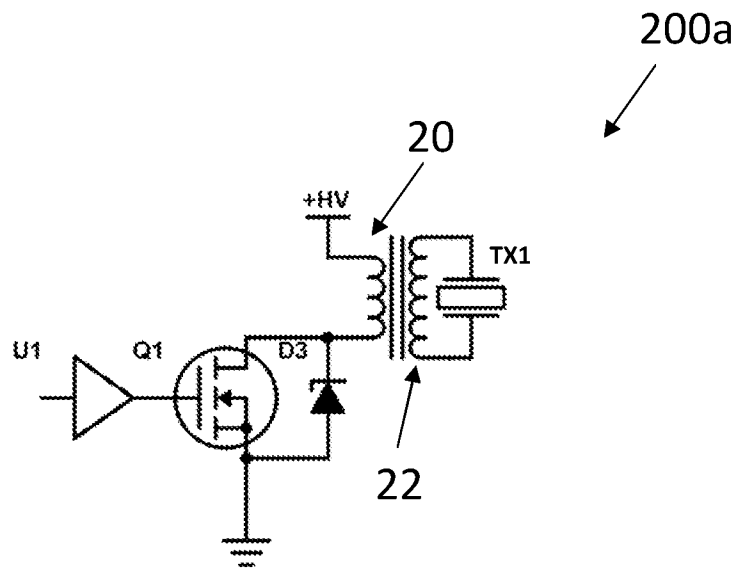


FIG. 2C

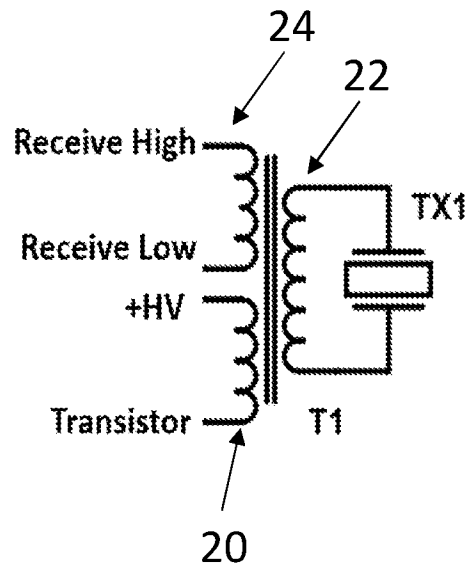


FIG. 2D

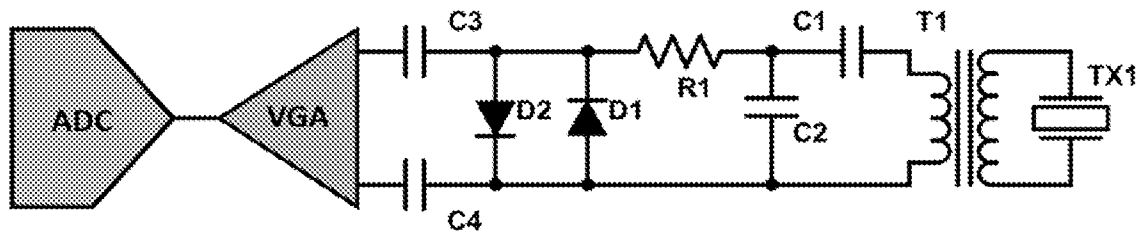


FIG. 3A

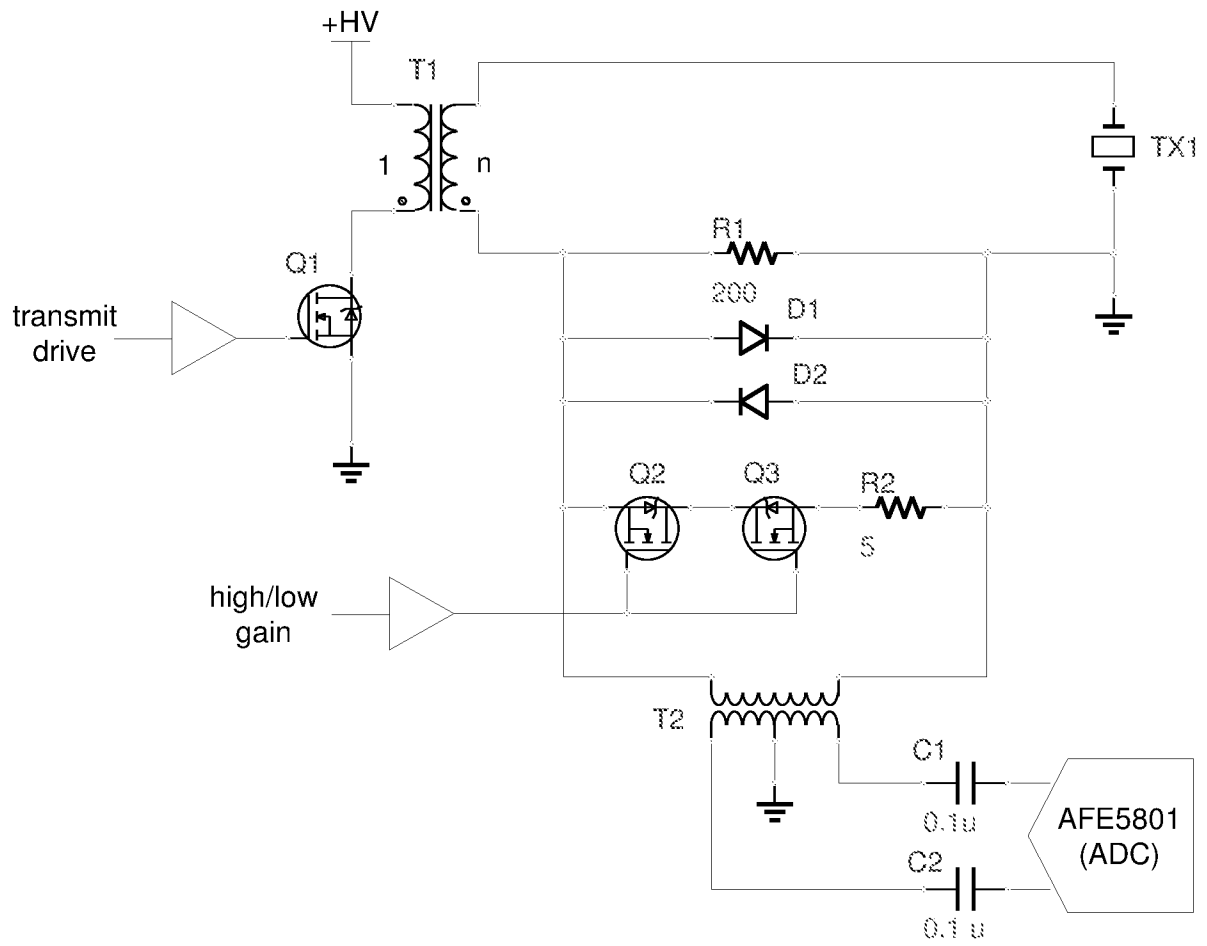
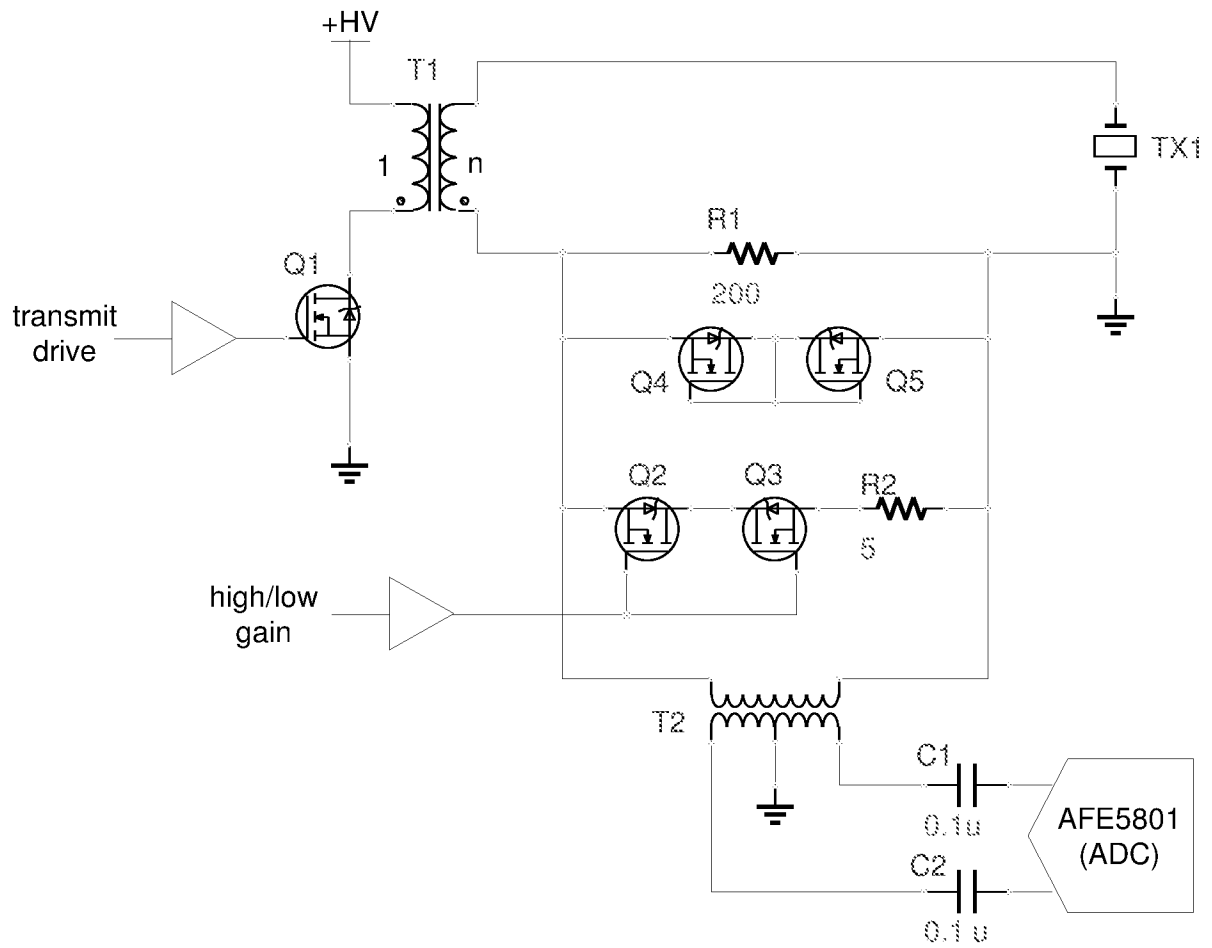


FIG. 3B





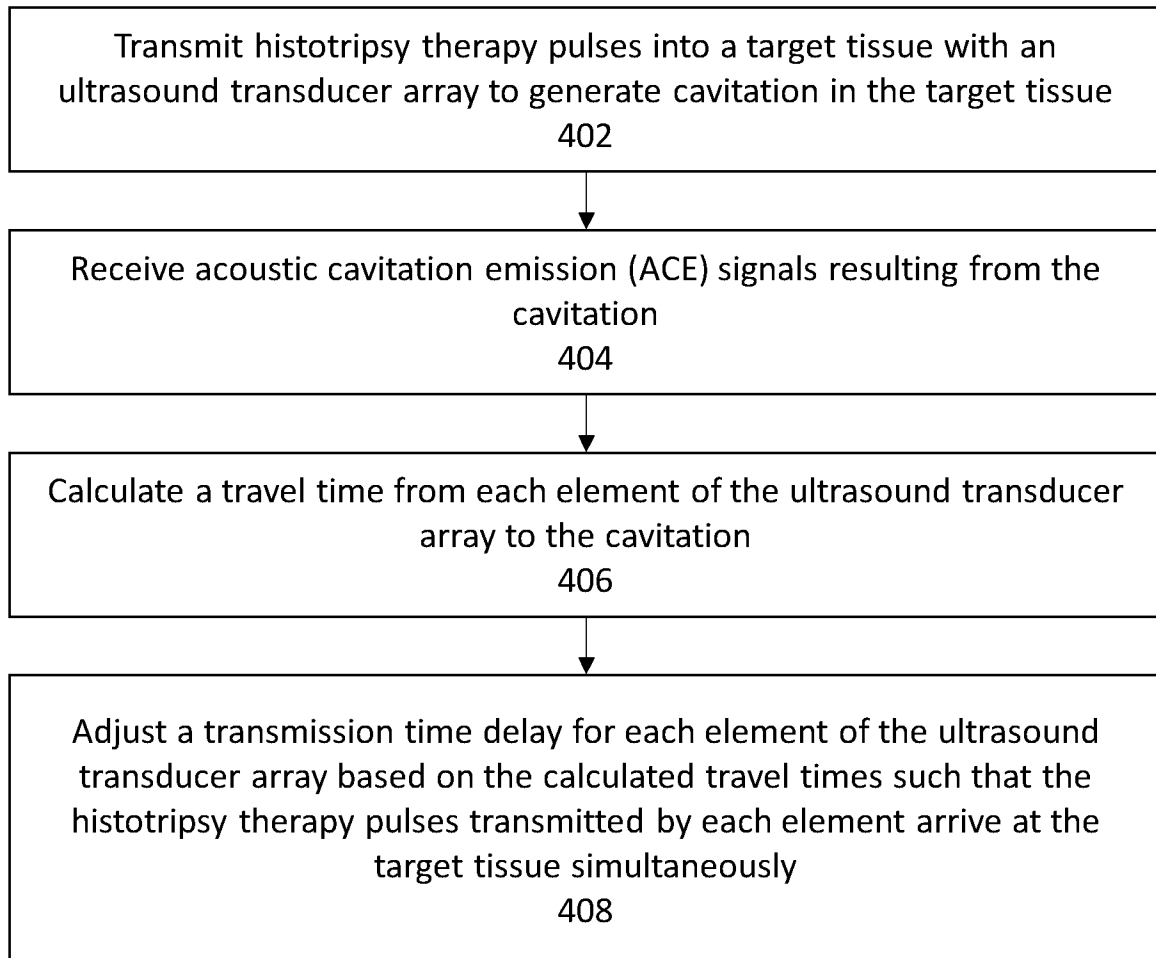
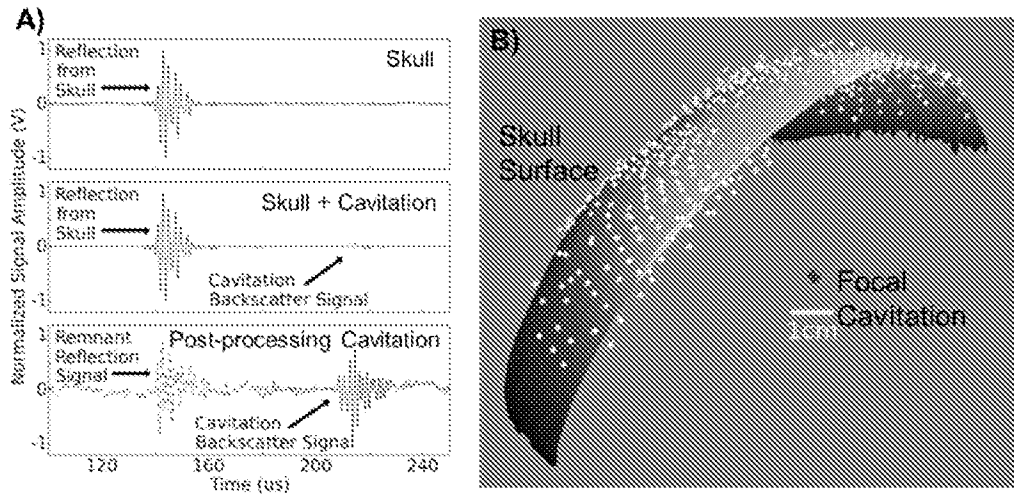
**FIG. 4**

FIG. 5



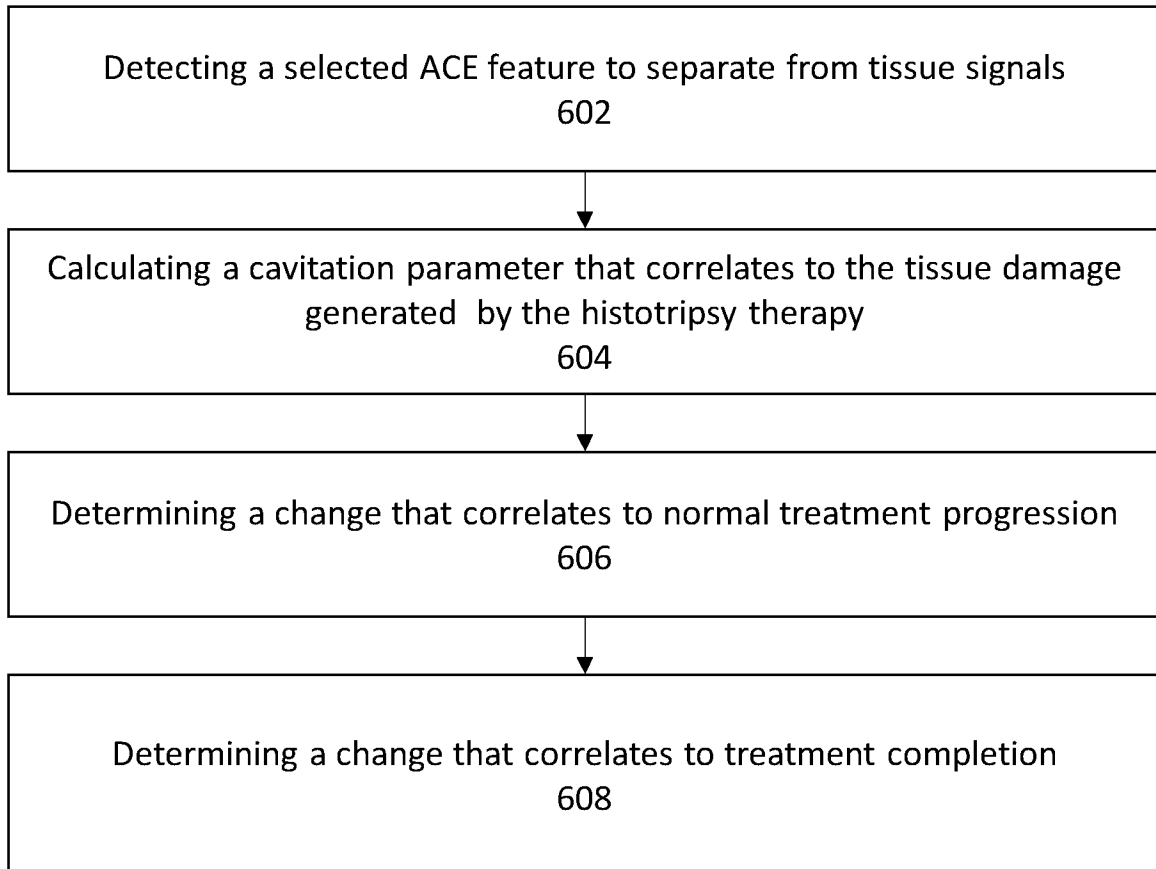
**FIG. 6**

FIG. 7

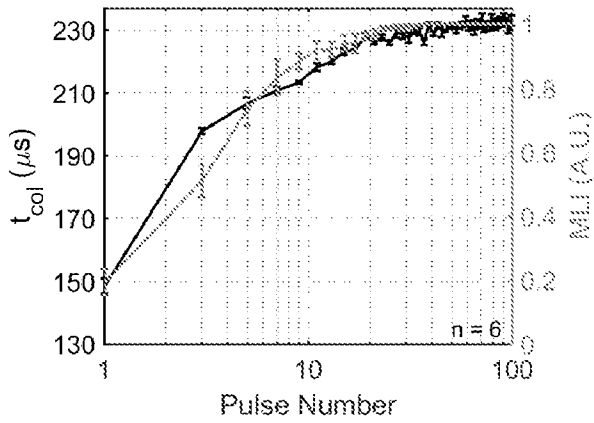


FIG. 8A

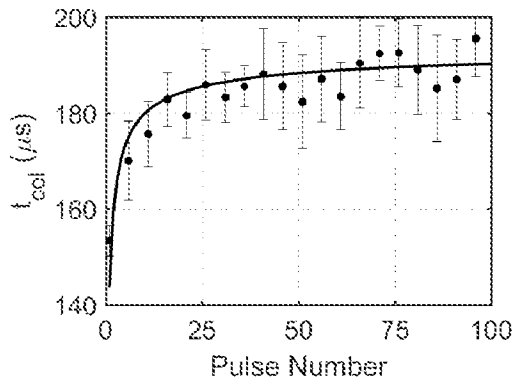


FIG. 8B

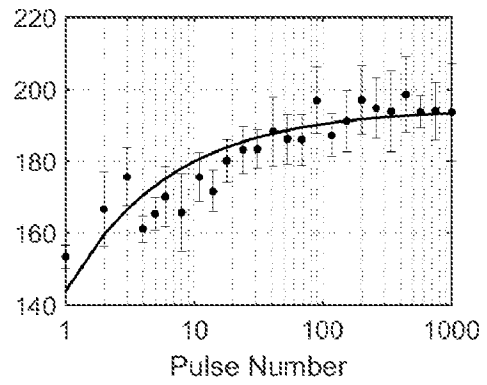


FIG. 9

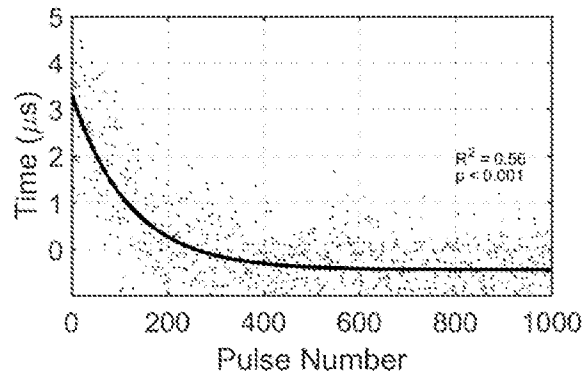
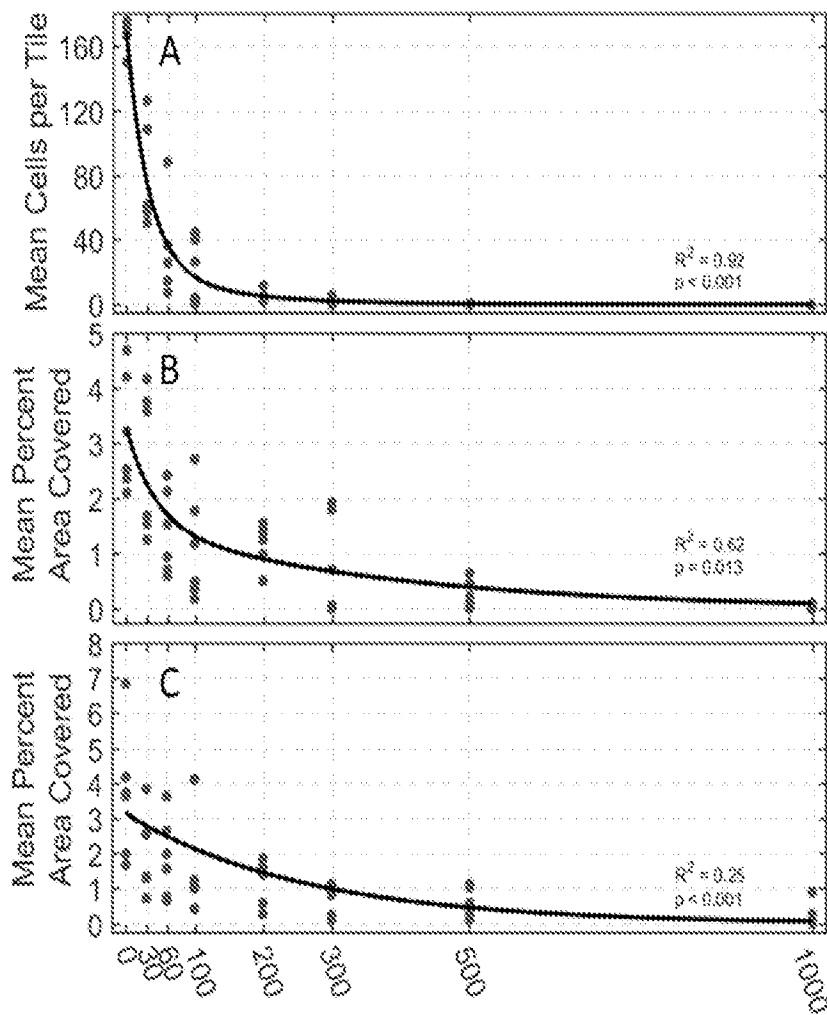


FIG. 10



WO 2022/047193

## INTERNATIONAL SEARCH REPORT

PCT/US2021/048008

International application No.

PCT/US 21/48008

<b>A. CLASSIFICATION OF SUBJECT MATTER</b> IPC - A61N 7/00; A61B 17/225 (2021.01)  CPC - A61N 7/00; A61B 17/225; A61B 2017/00172; A61B 2017/22007; A61N 2007/0065; A61N 2007/0039  According to International Patent Classification (IPC) or to both national classification and IPC		
<b>B. FIELDS SEARCHED</b>  Minimum documentation searched (classification system followed by classification symbols) See Search History document  Documentation searched other than minimum documentation to the extent that such documents are included in the fields searched See Search History document  Electronic data base consulted during the international search (name of data base and, where practicable, search terms used) See Search History document		
<b>C. DOCUMENTS CONSIDERED TO BE RELEVANT</b>		
Category*	Citation of document, with indication, where appropriate, of the relevant passages	Relevant to claim No.
Y --- A	US 2012/0010541 A1 (CAIN et al.) 12 January 2012 (12.01.2012), entire document, especially Fig. 1, para [0014], [0023], [0084], [0088], [0089], [0094], [0098], [0101], [0209], [0249], [0255], [0315]	37, 38 ----- 1-7
Y --- A	US 2020/0164231 A1 (HISTOSONICS, INC.) 28 May 2020 (28.05.2020), entire document, especially para [0116], [0121], [0124], [0147]	37, 38 ----- 1-7
A	MACOSKEY, "Acoustic Methods for Histotripsy Feedback." Diss. 2019. University of Michigan, published online 2019 (2019), Fig. 3.6; pg 83 [online] < <a href="https://deepblue.lib.umich.edu/handle/2027.42/149988">https://deepblue.lib.umich.edu/handle/2027.42/149988</a> > <DOI: <a href="https://hdl.handle.net/2027.42/149988">https://hdl.handle.net/2027.42/149988</a> >	1-7
X, P	US 2020/0346046 A1 (HISTOSONICS, INC.) 05 November 2020 (05.11.2020), entire document	1-7, 37, 38
<input type="checkbox"/> Further documents are listed in the continuation of Box C. <input type="checkbox"/> See patent family annex.		
* Special categories of cited documents: "A" document defining the general state of the art which is not considered to be of particular relevance "D" document cited by the applicant in the international application "E" earlier application or patent but published on or after the international filing date "L" document which may throw doubts on priority claim(s) or which is cited to establish the publication date of another citation or other special reason (as specified) "O" document referring to an oral disclosure, use, exhibition or other means "P" document published prior to the international filing date but later than the priority date claimed "T" later document published after the international filing date or priority date and not in conflict with the application but cited to understand the principle or theory underlying the invention "X" document of particular relevance; the claimed invention cannot be considered novel or cannot be considered to involve an inventive step when the document is taken alone "Y" document of particular relevance; the claimed invention cannot be considered to involve an inventive step when the document is combined with one or more other such documents, such combination being obvious to a person skilled in the art "&" document member of the same patent family		
Date of the actual completion of the international search 14 December 2021		Date of mailing of the international search report <b>JAN 21 2022</b>
Name and mailing address of the ISA/US Mail Stop PCT, Attn: ISA/US, Commissioner for Patents P.O. Box 1450, Alexandria, Virginia 22313-1450 Facsimile No. 571-273-8300		Authorized officer Kari Rodriguez  Telephone No. PCT Helpdesk: 571-272-4300

Continuation of Box No. III -- Observations where unity of invention is lacking

The inventions listed as Groups I-V do not relate to a single general inventive concept under PCT Rule 13.1 because, under PCT Rule 13.2, they lack the same or corresponding special technical features for the following reasons:

**Special Technical Features**

Group I includes the special technical feature of a transmit-receive switch, not included in the other groups.

Group II includes the special technical feature of, attenuate the incoming voltage signals, not included in the other groups.

Group III includes the special technical feature of, monitor treatment progression, not included in the other groups.

Group IV includes the special technical feature of, adjusting a transmission time delay, not included in the other groups.

Group V includes the special technical feature of, and overlaying the cavitation map onto an image, not included in the other groups.

**COMMON TECHNICAL FEATURES**

The only technical feature shared by Groups I-V that would otherwise unify the groups is, an ultrasound transducer array, or more histotripsy pulses, transmission electronics, receive electronics, transmitted and received signals. However, this shared technical feature does not represent a contribution over the prior art, because the shared technical feature is disclosed by US 2012/0010541 A1 to Cain et al. (hereinafter Cain).

The only technical feature shared by Groups I and II that would otherwise unify the groups is, a resistor. However, this shared technical feature does not represent a contribution over the prior art, because the shared technical feature is disclosed by Cain.

The only additional technical feature shared by Groups I and III-V that would otherwise unify the groups is, receive electronics configured to receive acoustic cavitation emissions from the cavitation. However, this shared technical feature does not represent a contribution over the prior art, because the shared technical feature is disclosed by Cain.

The only additional technical feature shared by Groups I, III, IV, and V that would otherwise unify the groups is, transmitting high-voltage histotripsy therapy pulses into a target tissue with transmit electronics and a histotripsy therapy transducer array to generate cavitation in the target tissue; receiving low-voltage acoustic cavitation emission signals from the cavitation with receive electronic. However, this shared technical feature does not represent a contribution over the prior art, because the shared technical feature is disclosed by Cain.

Cain discloses, an ultrasound transducer array (para [0098]- This would enable one to use high frequency ultrasound for initiation thus making use of the higher resolution of high frequency transducers or arrays), or more histotripsy pulses (para [0126]- the histotripsy process can be initiated by high-intensity pulses and maintained by low intensity pulses), transmission electronics (para [0249]- The array driving system, consisting of channel driving circuitry, associated power supplies (Model 6030A, HP, Palo Alto, Calif. USA), and a software platform to synthesize driving patterns), receive electronics (para [0101]- a separate transducer to ping (send an interrogation pulse or pulses) and a transducer to receive it; optical processes wherein optical scattering from the microbubbles (when initiated) is detected), a resistor (para [0255]- The resistor was used to convert the photodiode output from a current to a voltage), transmitted and received signals (para [0014]- The present disclosure provides methods for controlled mechanical subdivision of soft tissue that can include actuating a transducer to output an initiation pulse sequence; para [0023]- outputting a signal representative of attenuation of the bubble cloud, the methods further including receiving and monitoring the signal and adjusting the bubble cloud sustaining sequence in response to the signal), receive electronics configured to receive acoustic cavitation emissions from the cavitation (para [0264]- A hydrophone (Model 8103, Bruel and Kjr, Naerum, Denmark) with a frequency range of 0.1 Hz-180 kHz was placed outside the erosion zone to receive the acoustic emission of the bubble cloud), transmitting high-voltage histotripsy therapy pulses into a target tissue with transmit electronics and a histotripsy therapy transducer array to generate cavitation in the target tissue (para [0089]- Pulsed cavitation ultrasound therapy, or the histotripsy process according to the present teachings, can include four sub-processes, namely: initiation, maintenance, therapy, and feedback; para [0315]- Using a five cycle pulse, the measured peak negative pressure was 25 MPa for the voltage setting used for ultrasound treatments on liver tissue); receiving low-voltage acoustic cavitation emission signals from the cavitation with receive electronic (para [0213]- The acoustic backscatter signal was the output voltage of the 5-MHz monitoring transducer).

As the common features were known in the art at the time of the invention, they cannot be considered special technical features that would otherwise unify the groups.

Therefore, Groups I-V lack unity under PCT Rule 13.